RSC Advances

REVIEW

View Article Online
View Journal | View Issue

Cite this: *RSC Adv.*, 2026, **16**, 23684

Recent advances in π-conjugated organic thermoelectric materials: molecular design, properties, and applications

Mani Rajasekar *

Received 13th February 2026
Accepted 21st April 2026

DOI: 10.1039/d6ra01275b

rsc.li/rsc-advances

Organic thermoelectric materials have emerged as promising candidates for sustainable energy conversion due to their flexibility, low cost, and tunable molecular structures. This review highlights recent advances in π-conjugated systems based on fullerene, perylene, pyrrole, and thiophene derivatives. Molecular engineering strategies, including doping control, side-chain modification, and nanocomposite formation, are discussed to enhance electrical conductivity and Seebeck coefficient. Fullerene systems demonstrate exceptional n-type behavior and interfacial tunability. Perylene derivatives enable air-stable n-type performance with high power factors. Pyrrole-based polymers show improved thermoelectric efficiency through structural ordering and hybridization. Thiophene-based materials exhibit high carrier mobility and versatile molecular design for optimized energy conversion. Overall, these advances provide valuable design guidelines for next-generation flexible thermoelectric devices and waste heat recovery applications.

1. Introduction

The ever-increasing global demand for energy, coupled with rapid industrialization and technological advancement, has intensified concerns regarding fossil fuel depletion and environmental pollution.[1] A significant fraction of energy generated worldwide is dissipated as waste heat during industrial processes, power generation, and electronic operations. Recovering this low-grade waste heat and converting it into usable electrical energy represents a promising strategy to enhance energy efficiency and reduce carbon emissions. Thermoelectric (TE) materials, which enable direct heat-to-electricity conversion *via* the Seebeck effect and *vice versa* through the Peltier effect, have therefore attracted considerable attention as

Centre for Molecular and Nanomedical Sciences, International Research Centre, Sathyabama Institute of Science and Technology (Deemed to be University), Chennai-600 119, Tamil Nadu, India. E-mail: mrajasekar_83@yahoo.com; drmrajasekar.irc@sathyabama.ac.in

Mani Rajasekar

Dr M. Rajasekar is currently serving as Scientist-C/Assistant Professor (Research) in Organic Chemistry at the Centre for Molecular and Nanomedical Sciences, International Research Centre, Sathyabama Institute of Science and Technology (Deemed to be University), Chennai. He received his BSc in Chemistry from Arignar Anna Government Arts College (University of Madras) in 2005, MSc from C. Abdul Hakeem College (Thiruvalluvar University) in 2007, and MPhil from The New College (University of Madras) in 2008. He was awarded a PhD in Organic Chemistry from the University of Madras in 2015 and subsequently served as a National Postdoctoral Fellow (DST-SERB) from 2016 to 2018. His additional academic qualifications include BEd (2021) and MEd (2023) from Arunachala College of Education, affiliated with Tamil Nadu Teachers Education University. He has held academic positions including Visiting Lecturer at Anna University, Chennai. His research interests lie primarily in the field of material science, with a focus on organic and nanostructured materials. He has received several prestigious recognitions including NET, SLET, SET, NPDF, DSKPDF, Nehru PDF, and the Young Scientist Award. He has also been honored with the Best Researcher Award and the National Educational Star Award by the Glorious Organization for Accelerated to Literacy (GOAL), New Delhi. He has been recognized among the World's Top 2% Scientists in Organic Chemistry by Stanford University, underscoring his global research impact. He serves as a reviewer for RSC Advances and is the author of a highly cited review article published in the Chemical Engineering Journal (Impact Factor 13.8). His contributions include eight patents, sixteen authored books, and three scientific monographs, significantly advancing the fields of Organic Materials, Nanoscience, and Education.

solid-state energy conversion systems.[2] The performance of thermoelectric materials is evaluated by the dimensionless figure of merit, $ZT = S^2\sigma T/\kappa$, where S is the Seebeck coefficient, σ is the electrical conductivity, T is the absolute temperature, and κ is the thermal conductivity. Achieving a high ZT requires simultaneous optimization of these interdependent parameters, which remains a fundamental challenge. Conventional inorganic materials such as Bi_2Te_3, PbTe, and SiGe alloys exhibit high ZT values but suffer from limitations including high cost, toxicity, elemental scarcity, and mechanical rigidity. These drawbacks have motivated the exploration of alternative materials that are cost-effective, environmentally benign, and compatible with flexible and large-area device fabrication. Importantly, reported thermoelectric parameters are highly sensitive to measurement conditions such as device architecture, temperature, doping level, and processing methods; therefore, comparisons across studies should be made cautiously, with emphasis on trends rather than absolute values.[3]

Organic thermoelectric materials have emerged as promising candidates due to their intrinsic advantages, including low thermal conductivity, lightweight nature, solution processability, and mechanical flexibility. Conducting polymers such as polyaniline and PEDOT:PSS are particularly attractive owing to their high electrical conductivity, tunable doping levels, and compatibility with scalable fabrication techniques.

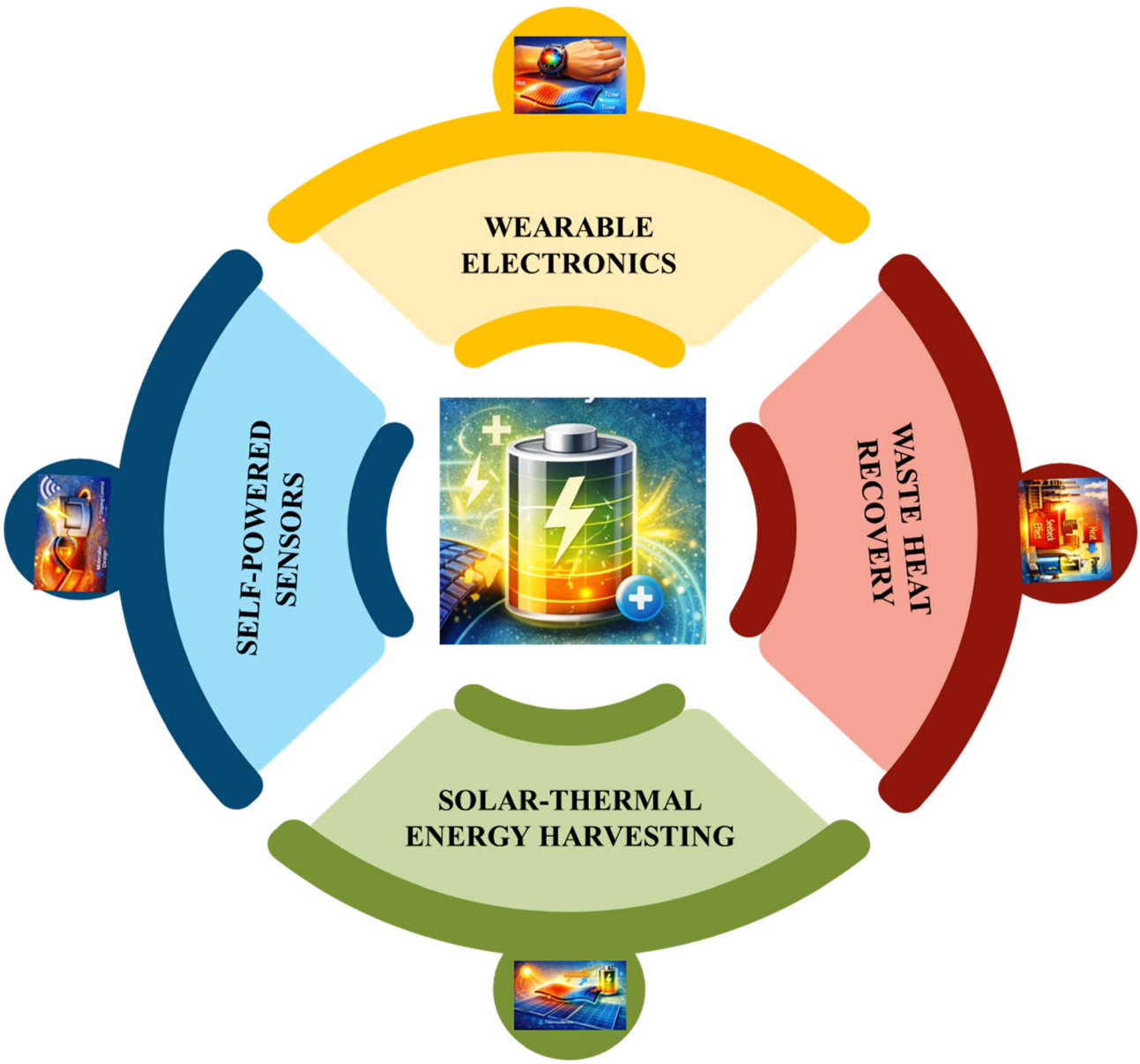

1

Fig. 1 Schematic representation of π-conjugated organic thermoelectric materials applications.

Their thermoelectric performance can be significantly enhanced through strategies such as secondary doping, structural ordering, and nanocomposite formation with carbon-based materials. These features make organic systems highly suitable for flexible and wearable thermoelectric applications.[4] This review aims to establish a clear relationship between molecular design and thermoelectric performance in π-conjugated organic materials. Specifically, it focuses on analyzing recent advances, identifying structure–property correlations, and critically evaluating key challenges and limitations. Fullerene, perylene, pyrrole, and thiophene-based systems are selected due to their structural diversity and complementary charge transport characteristics, representing both n-type and p-type materials. Together, these classes provide a comprehensive platform for understanding and designing high-performance organic thermoelectric systems.[5–7]

To provide a coherent framework, the discussed materials are categorized based on charge transport mechanisms and structural configurations, including molecular junctions, bulk conjugated systems, nanocomposites, and flexible or hybrid devices. Although these platforms differ in scale and architecture, they are unified by common principles such as π-conjugated charge transport, energy level alignment, and interfacial charge transfer. This framework enables systematic comparison of how molecular structure, morphology, and interfaces influence thermoelectric performance across different systems.[8–10] To further enhance clarity and analytical depth, the figures and tables in this review are designed as comparative tools that highlight performance trends and structure–property relationships. Key thermoelectric parameters, including electrical conductivity, Seebeck coefficient, and power factor, are presented in a consistent format to facilitate cross-study evaluation. In addition, figure captions are written to be self-contained and informative, ensuring that visual elements effectively convey the underlying scientific insights.[11–13] Among organic thermoelectric materials, π-conjugated systems such as fullerenes, perylene diimides, polypyrroles, and thiophene-based polymers have attracted particular attention due to their delocalized electronic structures and tunable properties. Fullerene-based materials exhibit strong electron affinity and are widely explored as n-type systems, with performance governed by molecular orientation, electrode coupling, and interfacial interactions. Perylene derivatives offer excellent air stability and efficient electron transport due to their strong π–π stacking and deep LUMO energy levels, while molecular engineering strategies enable enhanced conductivity and thermopower. Conducting polymers such as polypyrrole provide good electrical conductivity and processability but often require structural optimization to overcome limitations in carrier mobility. Thiophene-based materials, including polythiophenes and their derivatives, exhibit high carrier mobility and structural tunability, enabling both p-type and n-type thermoelectric performance through advanced molecular design strategies.[14–16]

Beyond molecular design, nanocomposite engineering plays a critical role in improving thermoelectric performance. The incorporation of carbon nanotubes, graphene, and other nanostructured fillers enhances charge transport through percolation networks while maintaining low thermal conductivity. Interfacial effects such as energy filtering, carrier scattering, and phonon blocking further contribute to performance enhancement. These synergistic effects enable the development of high-performance, flexible, and multifunctional thermoelectric devices, including wearable and stretchable systems.[17,18] Despite significant progress, existing studies reveal inherent trade-offs between electrical conductivity, Seebeck coefficient, and thermal conductivity, and the influence of molecular architecture, doping strategy, and processing conditions remains complex. Moreover, variations in device configuration and measurement conditions hinder direct comparison across studies. Therefore, a critical and comparative evaluation of different material systems is essential to identify key design principles and performance limits.[19,20]

In this context, this review provides a systematic and comparative analysis of π-conjugated organic thermoelectric materials (**1**), emphasizing molecular design strategies, doping mechanisms, nanocomposite engineering, and structure–property relationships. By integrating insights across different material classes and highlighting key challenges, this work aims to establish rational guidelines for the development of next-generation high-performance organic thermoelectric materials for sustainable energy applications (Fig. 1).

2. Thermoelectric-based fullerene

The thermoelectric properties of molecular junctions formed by a Pt electrode and graphene contacted through covalently bound [60]fullerene derivatives were investigated using conducting-probe atomic force microscopy (c-AFM). The [60] fullerene derivatives (**2**) were attached to the graphene electrode *via* different linker configurations. The results reveal that the Seebeck coefficient of these junctions is enhanced by up to ninefold compared to that of Au–C_{60}–Pt molecular junctions. Furthermore, the thermopower exhibits either positive or negative values depending on the molecular binding geometry and the local position of the Fermi energy. These findings highlight the ability of graphene electrodes to effectively tune and enhance the thermoelectric response of molecular junctions, while also confirming the exceptional thermoelectric performance of [60]fullerene-based systems (Fig. 2a).[21] Molecular junctions provide a versatile platform for exploring thermoelectric transport at the nanoscale and offer valuable insights for the development of cost-effective and environmentally friendly organic thermoelectric materials. Although theoretical studies have suggested that transport resonances arising from discrete molecular energy levels play a crucial role in thermoelectric performance, direct experimental evidence has remained limited. In this context, single-molecule junctions based on the endohedral fullerene $Sc_3N@C_{80}$ (**3**) connected to gold electrodes were investigated using a scanning tunnelling microscope. The magnitude and sign of the thermopower were found to depend strongly on the molecular orientation and the applied mechanical pressure. The encapsulated Sc_3N cluster induces a sharp electronic resonance close to the Fermi level, whose energy position can be tuned by pressure. Consequently,

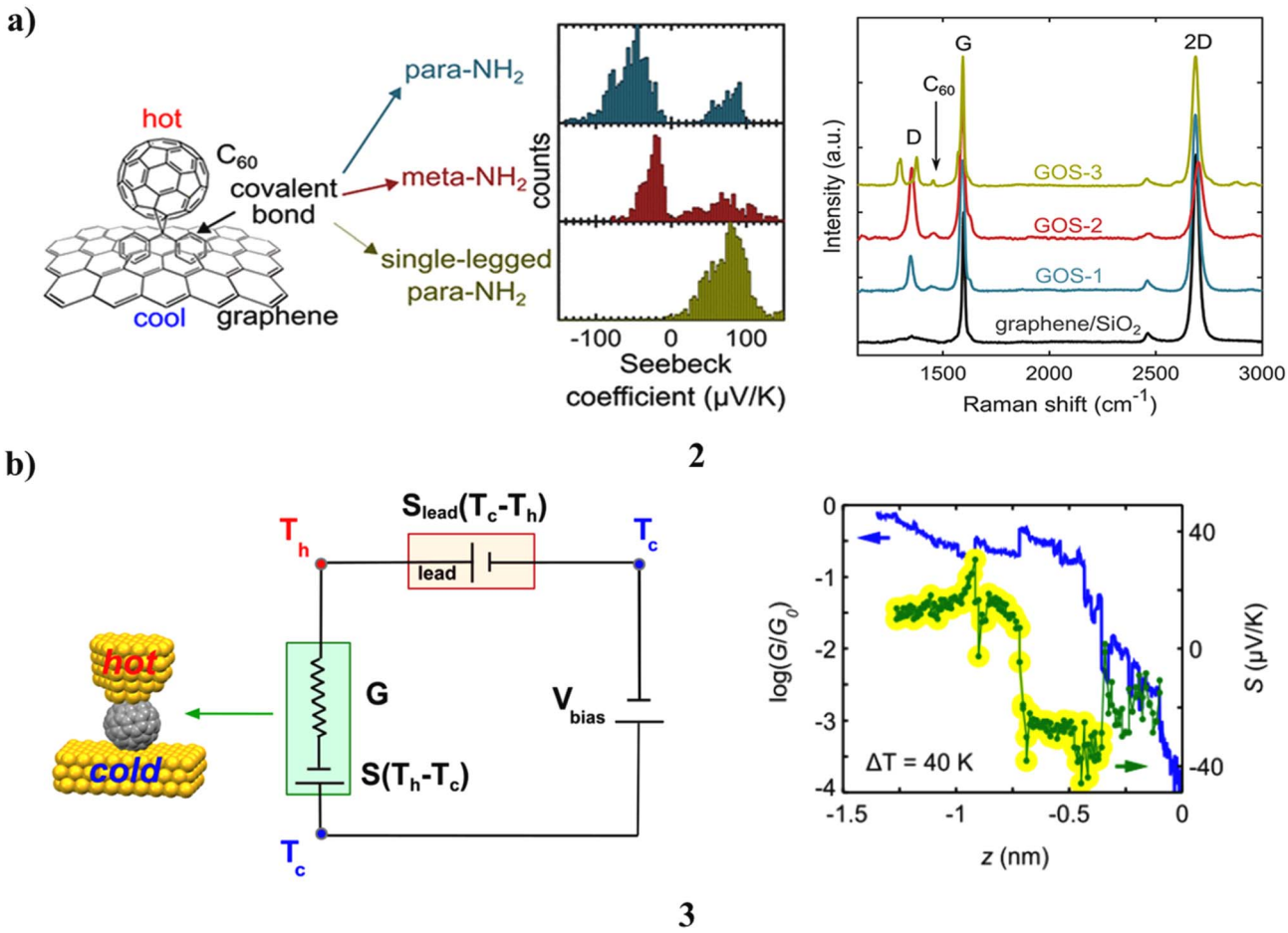

Fig. 2 (a) Enhanced thermoelectric response in metal-[60]fullerene-graphene molecular junctions (**2**) Reproduced from ref. 21 with permission from ACS Publisher, Copyright 2023. (b) Reversible bi-thermoelectric response in $Sc_3N@C_{80}$ driven by pressure-induced electronic tuning (**3**) Reproduced from ref. 22 with permission from Nature Publisher, Copyright 2016.

the thermopower can be reversibly modulated, exhibiting either positive or negative values. These findings identify $Sc_3N@C_{80}$ as a bi-thermoelectric material and provide direct experimental evidence for the critical role of transport resonances in molecular junctions (Fig. 2b).[22]

Nickel thin films containing nanovoids filled with fullerene (C_{60}) molecules (**4**) were successfully fabricated, and their thermoelectric properties were investigated from room temperature down to approximately 30 K. The underlying concept is to enhance phonon scattering at the C_{60}/Ni heterointerfaces to improve thermoelectric performance. The atomic distribution within the pristine Ni and Ni–C_{60} nanocomposite layers was analyzed using Auger electron spectroscopy depth profiling. Sample morphology and structural integrity were examined by cross-sectional scanning electron microscopy (SEM). The Seebeck coefficient and electrical conductivity were measured using an automated, custom-built experimental setup. Nanostructuring induced by Ar^+ ion treatment was found to significantly enhance the thermopower across the entire temperature range. Furthermore, filling the nanovoids with C_{60} led to an additional increase in thermopower below approximately 200 K. In several samples, the Seebeck coefficient increased by up to fourfold. This enhancement is attributed to increased charge carrier and phonon scattering at the Ni/C_{60} interfaces (Fig. 3a).[23] Sub-nanomaterials exhibit unique size-dependent properties that differ markedly from conventional nanomaterials, offering significant potential in catalysis, biomedicine, and sensing applications. However, their use in thermoelectrics has remained largely unexplored due to challenges such as poor thermal stability and low material yield. In this work, a series of thermoelectric composites was developed by incorporating highly thermally stable, commercially available fullerene sub-nanoclusters (**5**, C_{60}). The sub-nanoclusters act as an effective secondary phase, optimizing carrier concentration through interfacial charge transfer while significantly enhancing carrier mobility *via* orbital hybridization and size-dependent electrical scattering. Additionally, the intrinsically low thermal conductivity of C_{60}, arising from distorted chemical bonding and sub-nanometer pores, together with strong interfacial thermal resistance, effectively suppresses phonon transport. As a result, the 0.15 mol% $C_{60}/Bi_{0.4}Sb_{1.6}Te_3$ composite achieves an ultrahigh *ZT* of approximately 1.6 at 373 K, a thermoelectric conversion efficiency of about 7.4%, and a large cooling performance of nearly 73 K. These findings establish

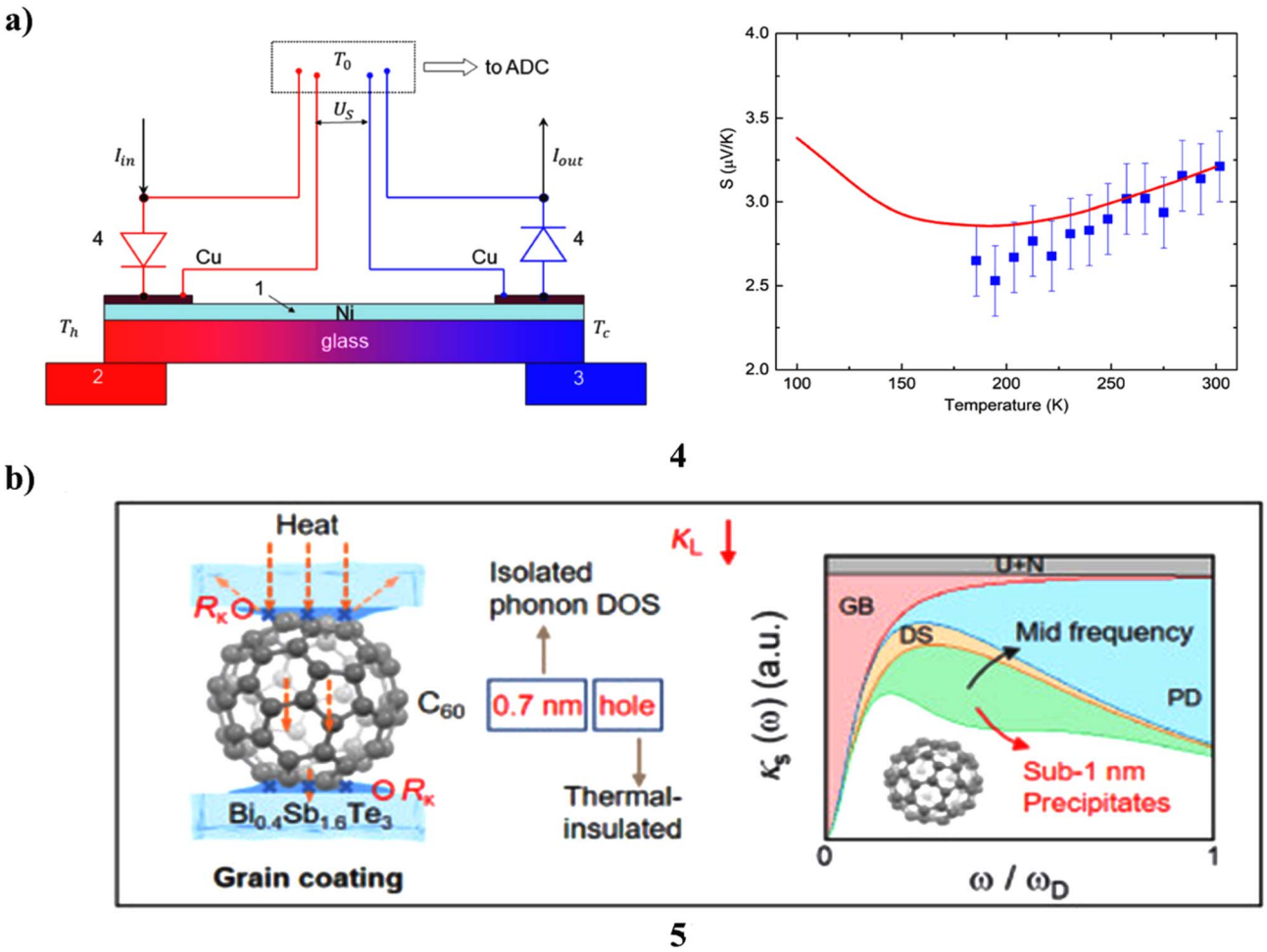

Fig. 3 (a) Nanostructure-induced thermoelectric enhancement in Ni–C_{60} films through interfacial scattering effects (4) Reproduced from ref. 23 with permission from MDPI Publisher, Copyright 2022. (b) High-performance bulk thermoelectric composites incorporating fullerene sub-nanoclusters (5) Reproduced from ref. 24 with permission from Elsevier Publisher, Copyright 2025.

sub-nanomaterials as promising components for thermoelectric applications and open new avenues in electronic devices, thermal management, and fullerene chemistry (Fig. 3b).[24]

A high-performance fullerene-based n-type doping system (6) has been developed for thermoelectric applications. By incorporating polar triethylene glycol (TEG) side chains into both the fullerene host material (PTEG-1) and the dopant (TEG-DMBI), excellent dopant–host miscibility is achieved in solution-processed films. Phase-imaging atomic force microscopy and coarse-grained molecular dynamics simulations confirm the improved morphological compatibility compared with films doped using commercially available N-DMBI. This enhanced miscibility results in a high doping efficiency of up to 18% at a dopant concentration of 20 mol%, leading to increased carrier density and mobility. The improved charge transport directly contributes to enhanced electrical conductivity. As a result, the doped PTEG-1 films exhibit an electrical conductivity of 1.81 S cm^{-1} and achieve a record-high power factor of 19.1 μW m^{-1} K^{-2}. These values represent one of the highest performances reported to date for solution-processable fullerene derivatives as n-type organic thermoelectric materials (Fig. 4a).[25] The effects of side-chain polarity and length on the n-type thermoelectric performance of a series of fullerene derivatives were systematically investigated. Fullerene derivatives (7) bearing either alkyl side chains or ethylene glycol (EG) side chains of varying lengths were employed as host materials for molecular doping. The results show that polar EG side chains provide superior miscibility with polar dopants compared to alkyl side chains, resulting in more than a fivefold enhancement in doping efficiency. In addition to doping efficiency, molecular order, another critical factor in thermoelectric performance can be effectively tuned through simultaneous control of side-chain polarity and length. Fullerene derivatives with appropriately sized polar side chains exhibit significantly enhanced Seebeck coefficients relative to their alkyl-substituted counterparts, likely due to improved miscibility and higher molecular ordering. Consequently, a maximum power factor of 23.1 μW m^{-1} K^{-2} is achieved for the fullerene derivative containing a tetraethylene glycol side chain. This performance ranks among the best reported for n-type organic thermoelectric materials. Moreover, EG side chains substantially improve the air stability of n-doped fullerene films. These findings provide

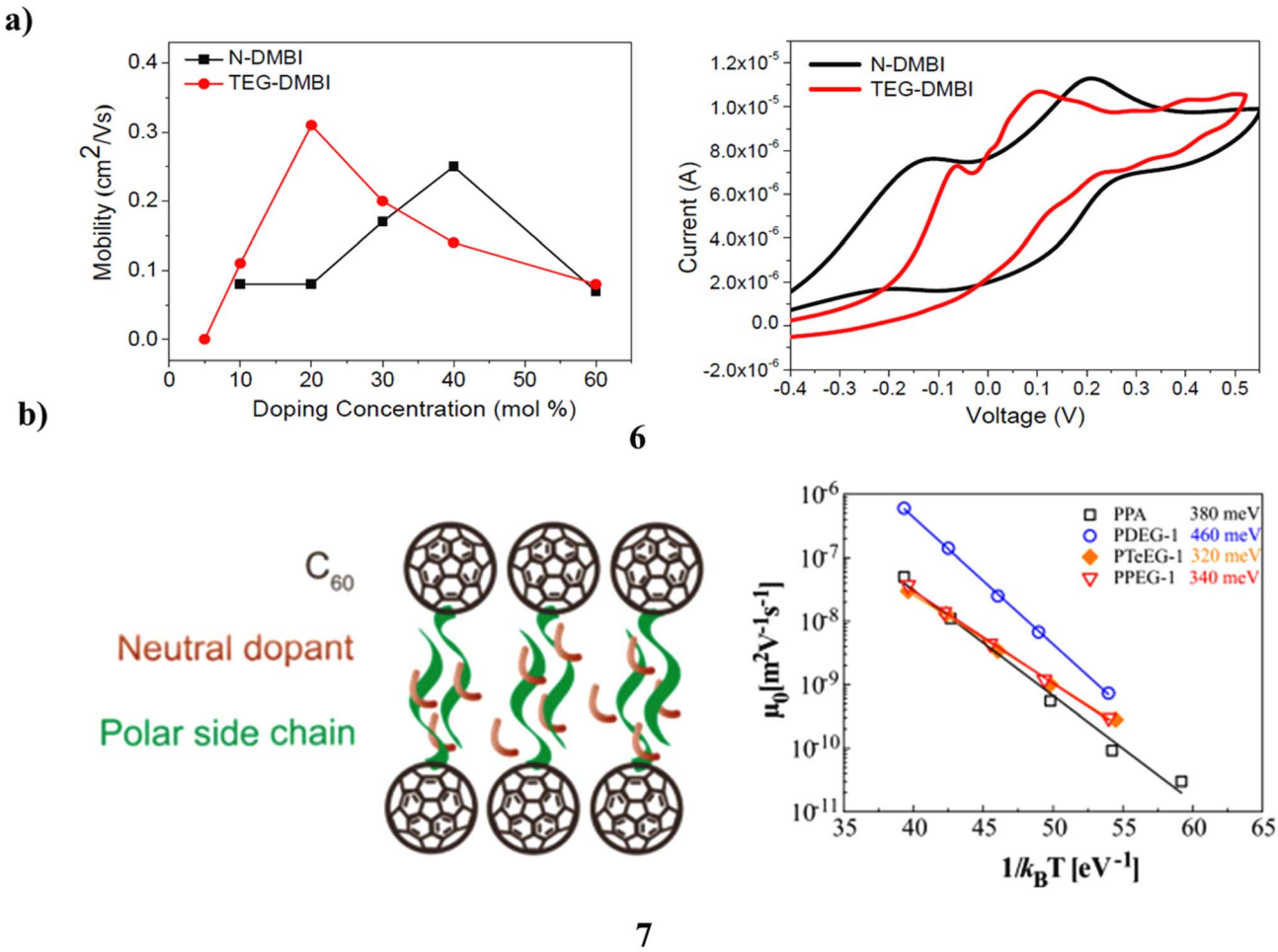

Fig. 4 (a) Host–dopant miscibility-driven enhancement of n-type thermoelectric properties in fullerene materials (**6**) Reproduced from ref. 25 with permission from RSC Publisher, Copyright 2017. (b) Side-chain-dependent doping efficiency and thermoelectric properties of fullerene derivatives (**7**) Reproduced from ref. 26 with permission from Elsevier Publisher, Copyright 2018.

valuable design guidelines for side-chain engineering in high-performance n-type small-molecule thermoelectrics (Fig. 4b).[26]

Constructing two-dimensional (2D) topological structures using nanoclusters such as fullerenes as fundamental building units remains a significant challenge. In this study, three types of bridged fullerene monolayers were designed, and a novel fullerene monolayer (**8**, α-C_{60}-2D) was comprehensively investigated using state-of-the-art first-principles calculations, guided by experimental synthesis. The results reveal that α-C_{60}-2D exhibits a direct band gap of 1.55 eV, in close agreement with experimental observations. The material shows pronounced optical linear dichroism with strong absorption in the long-wavelength ultraviolet region. Additionally, α-C_{60}-2D possesses a small anisotropic Young's modulus and a large hole mobility. Notably, an ultrahigh Seebeck coefficient is predicted at middle-to-low temperatures. These anisotropic optical, mechanical, electronic, and thermoelectric properties are attributed to the asymmetric bridging configurations between adjacent C_{60} clusters. Overall, this work highlights the promising potential of monolayer fullerene networks for applications across multiple functional material domains (Fig. 5a).[27] Density functional theory coupled with the non-equilibrium Green's function approach was used to analyze thermoelectric transport through C_{60} molecules (**9**) anchored to Al nano-electrodes. The study compares planar, pyramidal, and asymmetric surface geometries to understand structure-dependent transport behavior. The electrode geometry from planar to pyramidal leads to nearly a two-order reduction in electrical conductance (σ) and electronic thermal conductance (κ_{el}) due to weaker molecule–electrode coupling. Meanwhile, the Seebeck coefficient (S) decreases by about 55%, indicating strong configuration-dependent transport behavior. Among the three junctions, the asymmetric configuration exhibits the highest electronic thermoelectric figure of merit, with a maximum $Z_{el}T \approx 0.12$, assuming negligible phonon thermal conductance. In all C_{60} junctions, σ, κ_{el}, S, and $Z_{el}T$ increase with temperature, although the enhancement is minimal in the pyramidal junction owing to the large energy separation between the Fermi level and molecular frontier orbitals. Strain engineering further modulates thermoelectric performance, with S increasing sharply under tensile strain in the planar junction. In contrast, the asymmetric junction reaches its maximum Seebeck coefficient

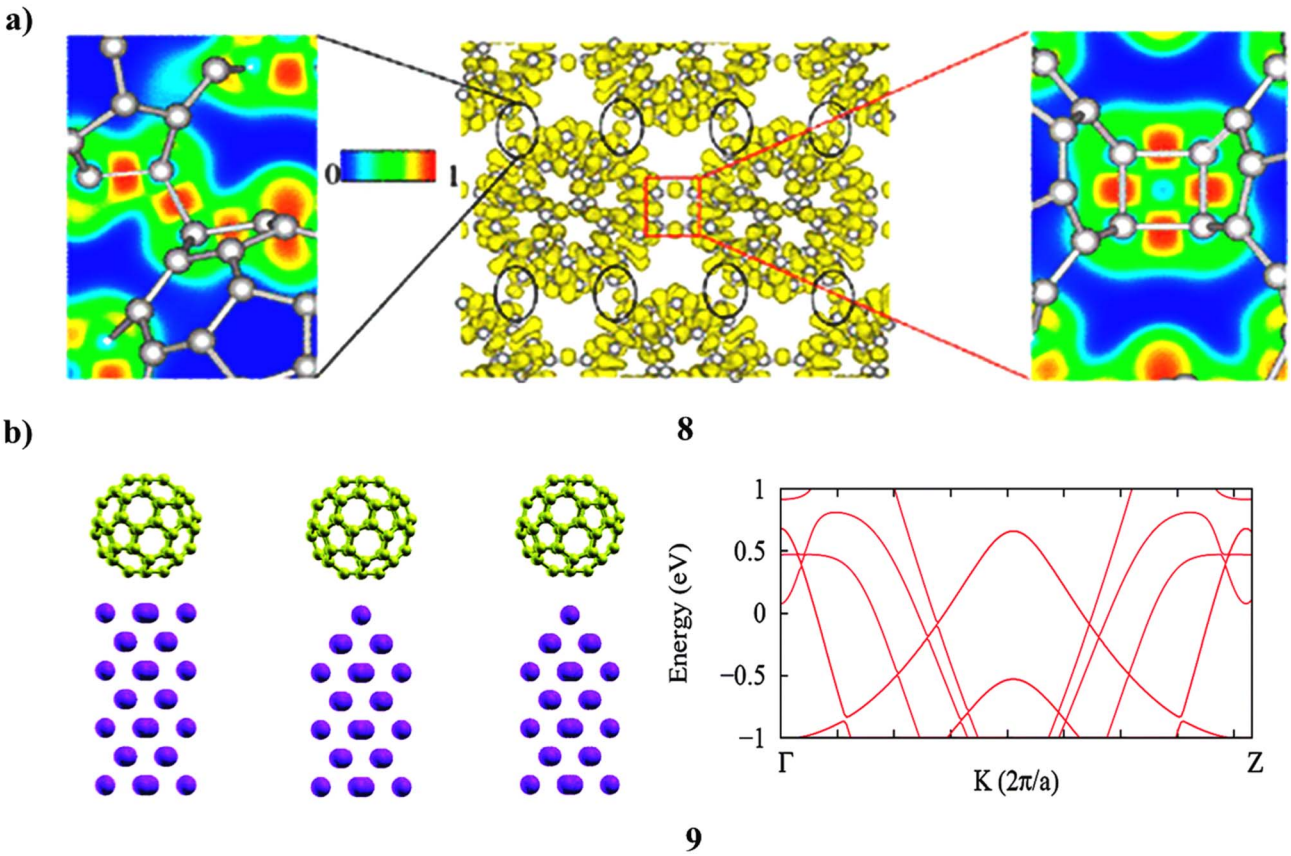

Fig. 5 (a) Thermoelectric properties of two-dimensional fullerene networks (**8**) Reproduced from ref. 27 with permission from ACS Publisher, Copyright 2022. (b) Thermoelectric transport properties of fullerene-based molecular junctions from first-principles calculations (**9**) Reproduced from ref. 28 with permission from RSC Publisher, Copyright 2016.

(S) at a tensile strain of 0.2 Å, while the pyramidal junction shows peak S under a compressive strain of −0.4 Å, demonstrating a clear strain-dependent thermoelectric response. These trends arise from the dependence of S on the slope and magnitude of the transmission spectrum near the Fermi level. Overall, shifting the Fermi level is identified as an effective strategy for maximizing $Z_{el}T$ in fullerene-based and other molecular junctions (Fig. 5b).[28]

Zigzag graphene nanoribbons (GNRs) were employed as electrodes to investigate the electron transport, optical, and thermoelectric properties of four molecular devices based on fullerene clusters (**10**). The current–voltage (I–V) characteristics under applied bias reveal pronounced multiple negative differential resistance (NDR) and platform effects, which are further elucidated through analyses of the density of states (DOS) and projected density of states (PDOS). Rotational studies of two distinct $(C_{60})_4$ molecular configurations confirm that both NDR and platform behaviors are intrinsic features of these devices. Photocurrent responses were evaluated at wavelengths corresponding to maximum optical absorption, demonstrating that α-$(C_{60})_4$ clusters linked by a [2 + 2] ring addition bond along the transport direction exhibit superior optical performance. In contrast, β-$(C_{60})_4$ clusters connected *via* single C–C bonds show comparatively weaker photoelectric response. Additionally, the thermoelectric currents of the devices were systematically analyzed. These findings deepen the understanding of charge transport and energy conversion in fullerene cluster-based systems and highlight their potential for applications in molecular electronics and optoelectronic devices (Fig. 6a).[29] The realization of two-dimensional (2D) C_{60}-based fullerene networks (**11**) with anisotropic and nanoporous lattices represents a significant advancement and opens new avenues for designing novel nanomaterials. Theoretical calculations were performed to predict and systematically evaluate the stability and physical properties of previously unexplored C_{60}-based lattices. Energy minimization of large structural configurations revealed a variety of stable 2D, 1D, and porous carbon networks with energies comparable to that of isolated C_{60} cages. Density functional theory calculations confirm that these networks exhibit excellent thermal stability and display metallic, semiconducting electronic behavior depending on their atomic arrangements. Machine-learning-based interatomic potentials were further employed to investigate the thermal and mechanical properties of the nanoporous 2D lattices. The predicted lattice thermal conductivity of the quasi-hexagonal C_{60} phase shows excellent agreement with experimental data, with anisotropic room-temperature values on the order of 10 W m^{-1} K^{-1}. Notably, unlike most carbon-based 2D materials, C_{60}

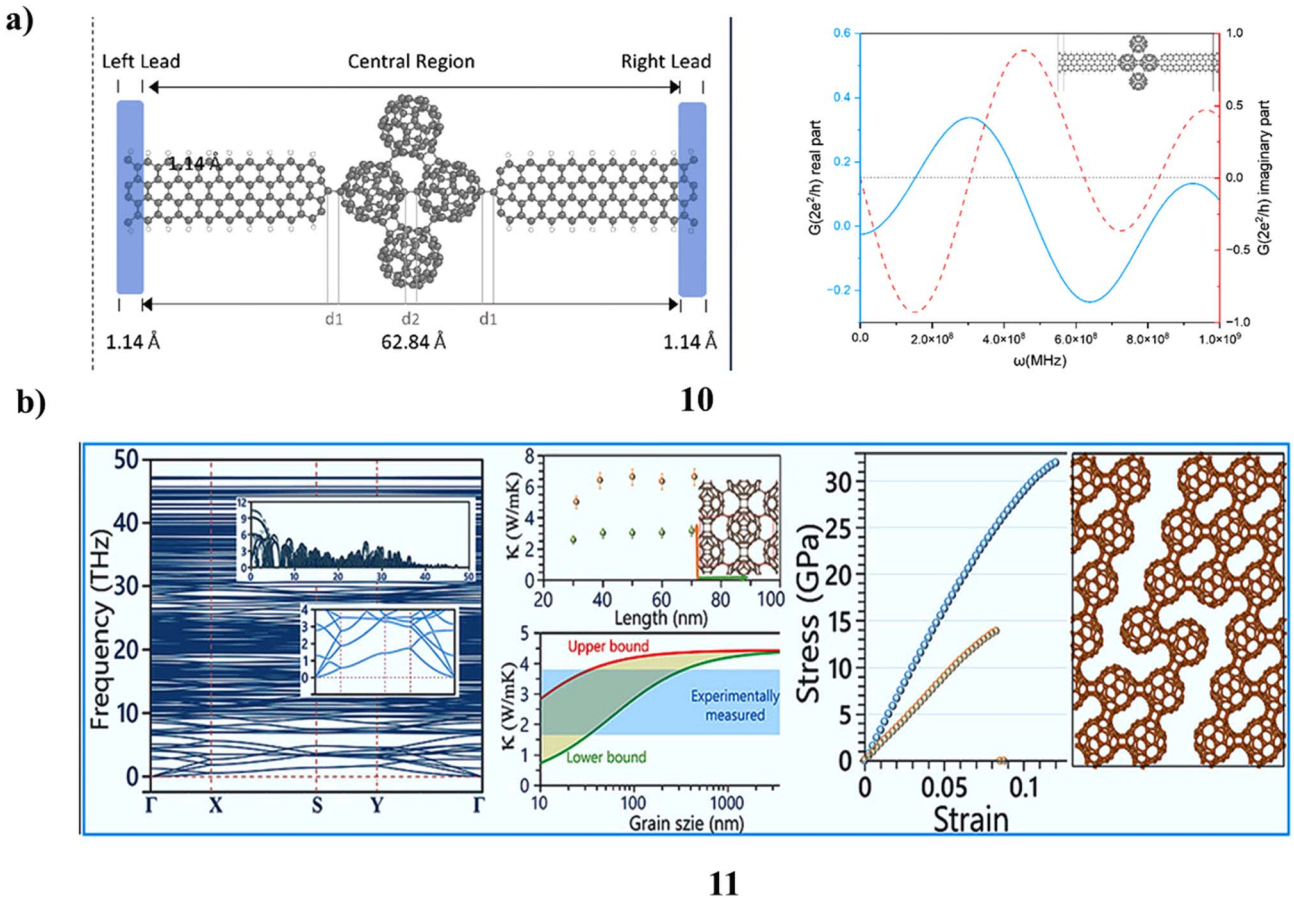

Fig. 6 (a) Structural and electronic properties of fullerene cluster-based molecular devices with graphene nanoribbon electrodes (**10**) Reproduced from ref. 29 with permission from RSC Publisher, Copyright 2023. (b) Structural and mechanical characteristics of C_{60}-based two-dimensional fullerene networks (**11**) Reproduced from ref. 30 with permission from Elsevier Publisher, Copyright 2023.

nanosheets are predicted to exhibit positive thermal expansion coefficients. Additionally, porous C_{60}-based networks demonstrate outstanding mechanical performance, with tensile strength and elastic modulus reaching approximately 50 GPa and 300 GPa, respectively (Fig. 6b).[30]

Solution-printable and flexible thermoelectric materials are highly attractive for scalable fabrication and powering next-generation flexible electronics; however, achieving mechanical flexibility alongside excellent thermoelectric performance remains challenging, particularly for n-type systems. Two-dimensional TiS_2 nanosheets (**12**) were exfoliated from layered polycrystalline powders and integrated with C_{60} nanoparticles to construct a novel hybrid system, resulting in a flexible n-type thermoelectric material with enhanced performance potential. The resulting C_{60}/TiS_2 hybrid films exhibit simultaneous enhancement of the power factor and suppression of thermal conductivity. As a consequence, a high thermoelectric figure of merit of $ZT \approx 0.3$ is achieved at 400 K, significantly outperforming previously reported solution-printable and flexible n-type TE materials. Notably, this performance is comparable to that of single-crystal TiS_2-based thermoelectrics, which are costly, difficult to fabricate, and incompatible with solution processing. Furthermore, the C_{60}/TiS_2 hybrid dispersion can be used as a printable ink to fabricate large-area flexible TE devices. An impressive output power density of 1.68 W m^{-2} is generated under a temperature gradient of 20 K. Overall, this work establishes a promising strategy for developing high-performance, solution-printable thermoelectric materials for flexible electronic applications (Fig. 7a).[31] A series of fullerene-C_{60}-PEDOT hybrid polymers (**13**) with varying C_{60} contents was successfully synthesized and characterized using UV, TGA, XRD, and TEM. These hybrids were covalently grafted onto the surface of C_{60}, enabling uniform dispersion of the fullerene units throughout the polymer network. The thermoelectric properties of the resulting hybrid films were examined both in the dark and under visible light irradiation. Under dark conditions, pristine PEDOT films (0.00 wt% C_{60}) exhibited an electrical conductivity of 240 ± 5 S cm^{-1} and a Seebeck coefficient of 10 ± 0.6 μV K^{-1}. Notably, the hybrid films showed pronounced light-responsive thermoelectric behavior, with the power factor in the dark reduced to approximately one-quarter of that measured under visible light. This strong light-inhibited effect demonstrates that the thermoelectric performance of fullerene-C_{60}-PEDOT hybrid polymers can be effectively and reversibly tuned through visible light irradiation, offering new opportunities for optically controllable thermoelectric devices (Fig. 7b).[32]

Solar-thermal evaporators are essential for interfacial solar-driven water evaporation, yet conventional systems often lack

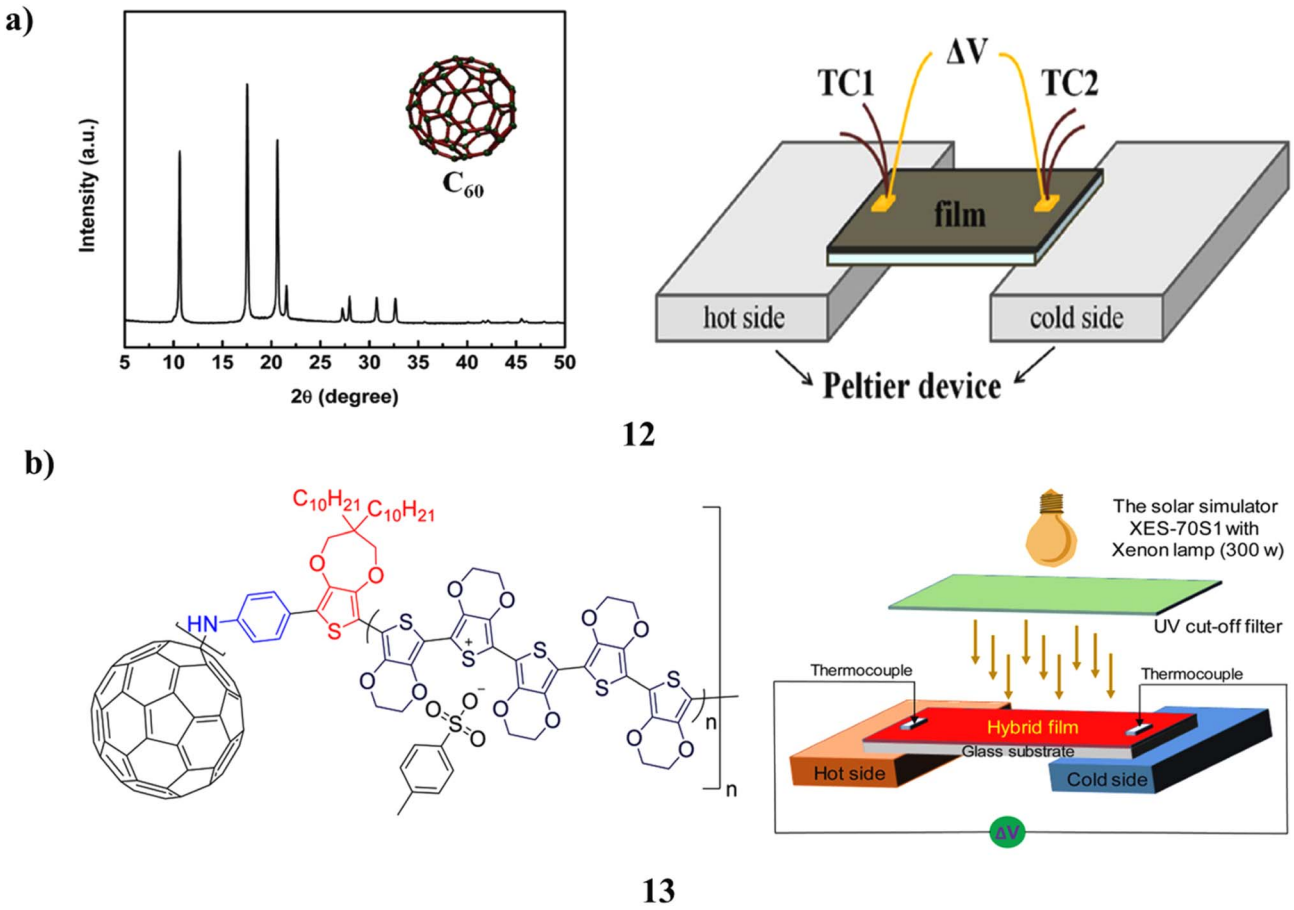

Fig. 7 (a) Solution-processable flexible n-type thermoelectrics based on fullerene/TiS_2 hybrid films (**12**) Reproduced from ref. 31 with permission from RSC Publisher, Copyright 2018. (b) Photoresponsive thermoelectric behavior of fullerene-C_{60}-PEDOT hybrid polymers (**13**) Reproduced from ref. 32 with permission from ACS Publisher, Copyright 2020.

integrated thermal management and efficient water transport, limiting their desalination performance. In this study, a solution-processable fullerene derivative (**14**, PCBM) was employed as a photothermal material due to its ester functional groups and achieved a photothermal conversion efficiency of 14.65%. By blending poly(*N*-isopropylacrylamide) (PNIPAm) and polyvinyl alcohol (PVA) as a carrier matrix, a solar-thermal thermoresponsive hydrogel (STT/H) was developed. The temperature-induced deformation of STT/H enables synergistic thermal regulation and rapid water transport, leading to enhanced evaporation efficiency compared to conventional hydrogels. Under simulated solar irradiation of 1.0 kW m^{-2}, the evaporation rate reached 1.46 kg m^{-2} h^{-1}. Furthermore, the temperature gradient generated during evaporation was effectively harvested using a thermoelectric module, enabling simultaneous water-electricity cogeneration. Under one-sun illumination, STT/H demonstrated efficient solar-driven performance. It achieved a water evaporation rate of 0.93 kg m^{-2} h^{-1}. Simultaneously, it generated an output voltage of 57.9 mV. This work extends solution-processable fullerene-based materials into solar-driven desalination and introduces a novel thermoresponsive double-network hydrogel for efficient seawater desalination (Fig. 8a).[33] Single-molecule junctions based on C_{82}, Gd@C_{82}, and Ce@C_{82} were investigated using scanning tunnelling microscope break-junction measurements combined with first-principles transport calculations to explore thermoelectric transport at the atomistic level. All fullerene-based junctions (**15**) exhibit negative thermopower confirming n-type behavior with significantly enhanced thermopower observed for Gd@C_{82} and Ce@C_{82} compared to pristine C_{82} while maintaining similar conductance. Consequently, the Gd@C_{82} junction delivers the highest reported single-molecule power factor, attributed to electronic and geometric modifications induced by the encapsulated metal atoms (Fig. 8b).[34]

Fullerene-based thermoelectric materials operate on the principle of converting a temperature gradient into electrical energy *via* the Seebeck effect, where the unique closed-cage π-conjugated structure and high electron affinity of fullerenes enable efficient n-type charge transport. Their thermoelectric performance is governed by tunable molecular energy levels, interfacial charge transfer, and strong phonon scattering at fullerene-electrode or fullerene-matrix interfaces, leading to moderate electrical conductivity, relatively high Seebeck coefficients, and low thermal conductivity; in optimized molecular junctions and composites, enhanced power factors and *ZT* values have been reported. The detection mechanism relies on sensing

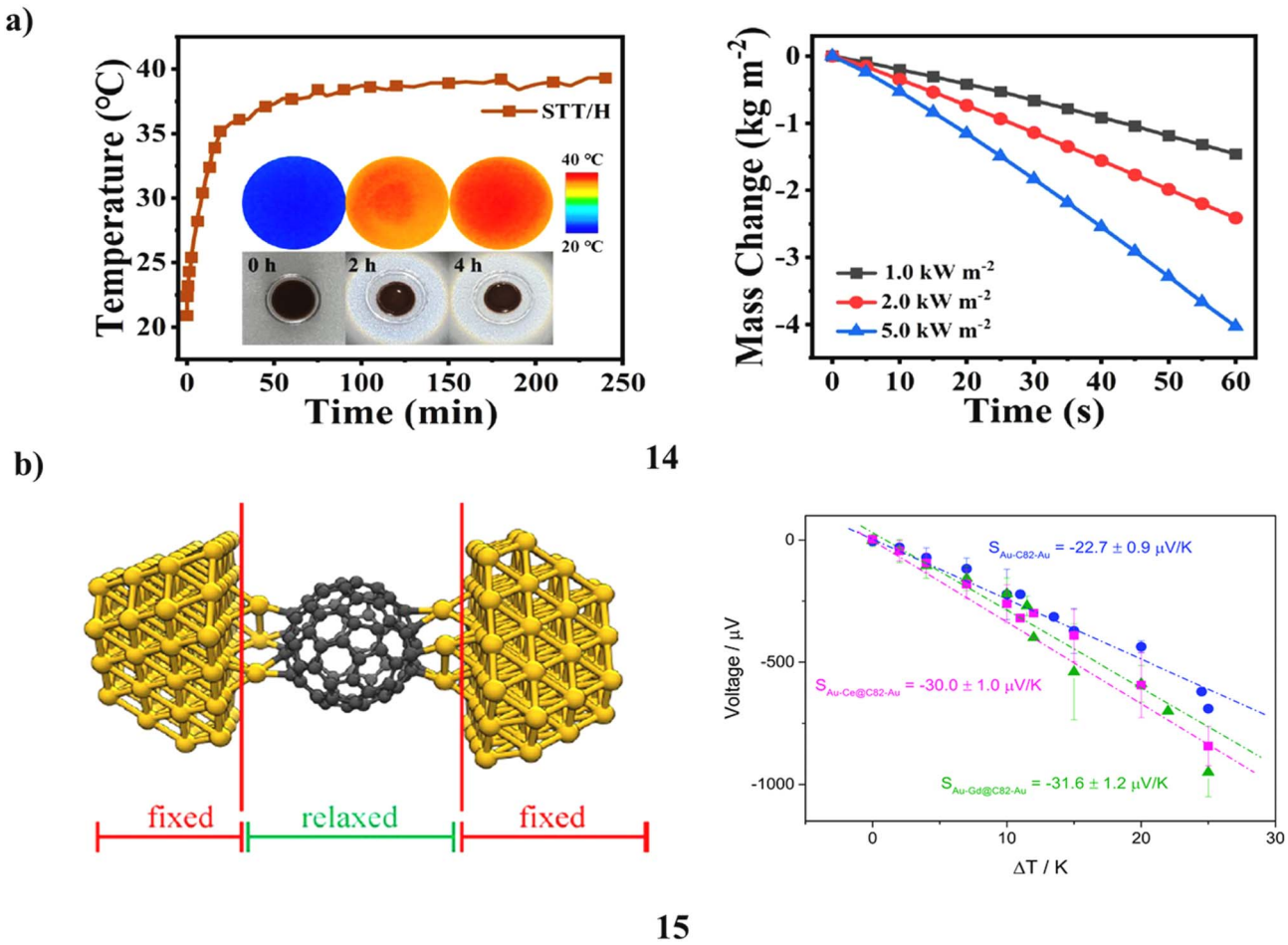

Fig. 8 (a) Solar-driven thermoresponsive hydrogel integrating photothermal conversion with thermoelectric power generation (**14**) Reproduced from ref. 33 with permission from RSC Publisher, Copyright 2025. (b) Large Seebeck effect in endohedral metallofullerene single-molecule junctions (**15**) Reproduced from ref. 34 with permission from RSC Publisher, Copyright 2015.

temperature differences through changes in voltage output or thermopower, which is highly sensitive to molecular orientation, electrode coupling, doping level, and Fermi-level alignment, allowing selective response to thermal stimuli rather than chemical species. Selectivity in fullerene systems mainly arises from controlled electronic structure, side-chain engineering, and host–dopant interactions that preferentially stabilize electron transport pathways. Key advantages include well-defined molecular structure, excellent electron transport, low thermal conductivity, tunable thermopower, compatibility with solution processing, and potential for flexible and nanoscale devices. However, disadvantages include relatively low intrinsic electrical conductivity compared to inorganic thermoelectrics, sensitivity of performance to interfacial and morphological disorder, challenges in large-area device integration, and stability issues under prolonged thermal or environmental stress, which still limit their widespread practical deployment.

3. Thermoelectric-based perylene

Doping plays a critical role in regulating charge transport and enhancing the performance of organic thermoelectric (TE) materials. In this study, a typical n-type organic semiconductor based on perylene diimide (**16**, PDI) was employed as a dopant to improve the thermoelectric properties of PEDOT:PSS films. At an optimal PDI content of 10 wt%, the electrical conductivity of PEDOT:PSS/PDI films reached 1500 S cm^{-1}, representing a 20% enhancement compared to pristine PEDOT:PSS. Simultaneously, the Seebeck coefficient increased significantly to 36.7 μV K^{-1}, corresponding to a 109% improvement. The enhanced thermoelectric performance is attributed to effective doping interactions between the lone-pair electrons of nitrogen atoms in PDI and the polarons in PEDOT chains. These interactions facilitate improved charge carrier transport within the polymer matrix (Fig. 9a).[35] The *N*-annulated perylene (NP)-based organic small molecules (**17**, OSMs) bearing di-*p*-tolylamine (DTA) and phenyl-di-*p*-tolylamine (PhDTA) end groups were synthesized and incorporated into single-walled carbon nanotubes (SWCNTs) to fabricate nanocomposite thin films for thermoelectric applications. The OSM/SWCNT weight ratios were varied from 1 : 1 to 1 : 4 to optimize performance. Owing to their planar molecular structures, both OSMs exhibit strong π–π interactions and efficient charge transfer with SWCNTs. In

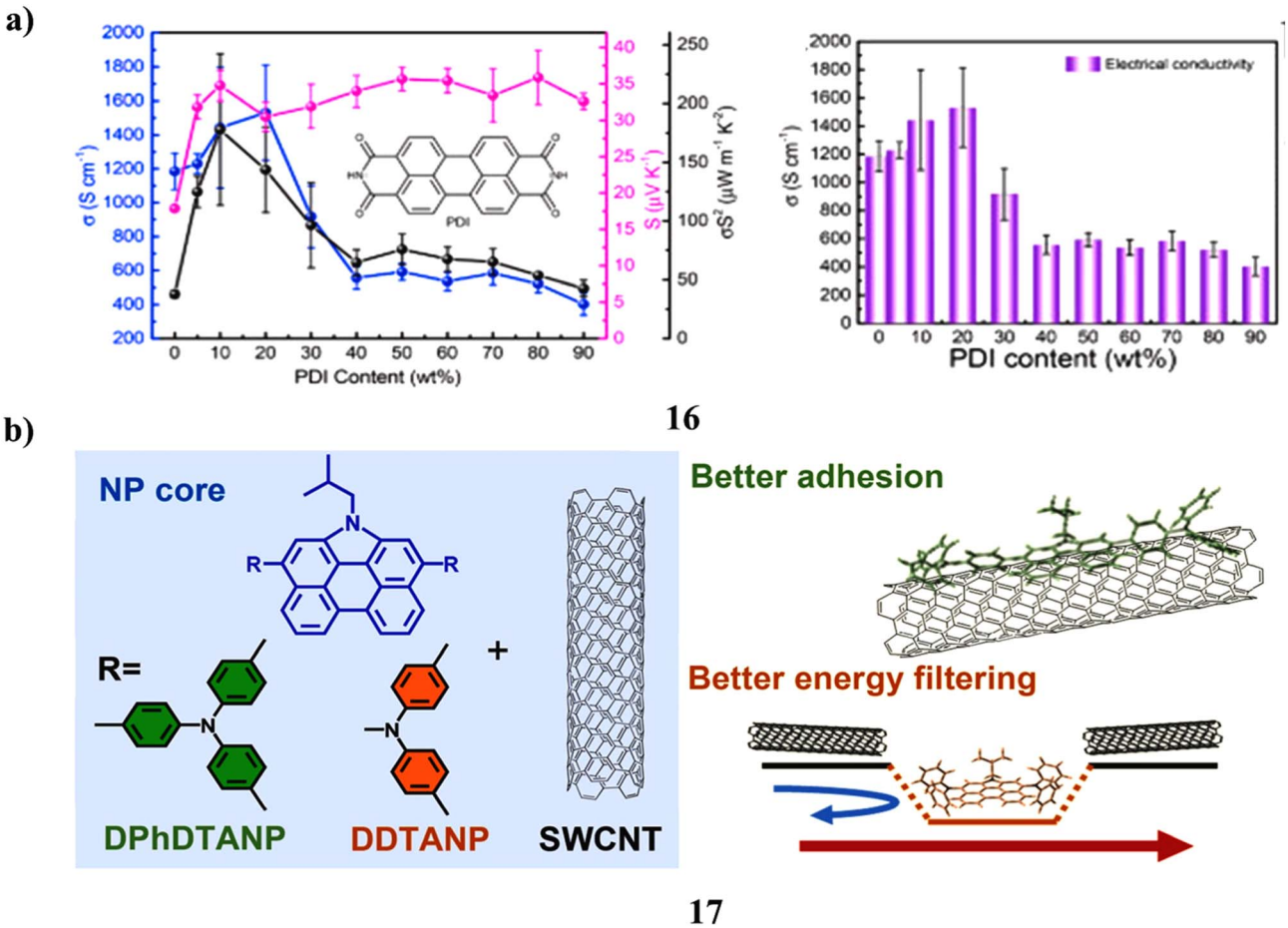

Fig. 9 (a) PDI doping-induced enhancement of thermoelectric performance in PEDOT:PSS films. (**16**) Reproduced from ref. 35 with permission from Elsevier Publisher, Copyright 2021. (b) High-performance thermoelectric behavior in perylene/SWCNT composites driven by efficient charge transfer (**17**) Reproduced from ref. 36 with permission from Elsevier Publisher, Copyright 2024.

particular, the DDTANP/SWCNT composites, featuring a lower HOMO energy level, promote pronounced energy filtering, resulting in an enhanced Seebeck coefficient. At an optimized ratio of 1 : 3, the DDTANP/SWCNT film achieves an electrical conductivity of 214.7 S cm^{-1} and a Seebeck coefficient of 59.8 μV K^{-1}. In contrast, the flatter DPhDTANP molecule improves interfacial adhesion and dispersion within the SWCNT network, leading to higher conductivity. Accordingly, the DPhDTANP/SWCNT (1 : 3) composite exhibits a conductivity of 256.4 S cm^{-1} and a Seebeck coefficient of 55.8 μV K^{-1}. The resulting power factor reaches 79.8 μW m^{-1} K^{-2}, surpassing that of the DDTANP/SWCNT composite. These results provide valuable insights into molecular design strategies for high-performance SWCNT-based thermoelectric composites (Fig. 9b).[36]

Organic thermoelectric materials have attracted increasing attention as environmentally friendly functional materials with strong potential for waste heat recovery. However, their development has been hindered by intrinsically low electrical conductivity. Incorporating single-walled carbon nanotubes (SWCNTs) into organic semiconductors has emerged as an effective strategy to enhance conductivity and overall thermoelectric performance. A radical-functionalized perylene diimide derivative (**18**, PDI-2T) with TEMPO substituents was rationally designed through molecular engineering and blended with SWCNTs to form organic thermoelectric composites. The resulting radical-containing composite films exhibit markedly superior thermoelectric performance compared to composites based on non-radical molecules. A maximum power factor of 278.2 ± 8.2 μW m^{-1} K^{-2} was achieved for p-type films, while n-type films reached 64.6 ± 13.5 μW m^{-1} K^{-2}. The enhanced performance is attributed to strengthened interactions between the radical molecules and SWCNTs, as well as optimized carrier concentrations within the composites. These findings introduce a new design paradigm for high-performance organic thermoelectric materials and devices (Fig. 10a).[37] Low-cost and environmentally benign organic thermoelectric materials are being developed as sustainable alternatives for waste-heat energy harvesting, though their performance is often limited by low Seebeck coefficients and a lack of efficient n-type systems. A highly crystalline, reduced perylene bisimide mixed ion-electron conductor (**19**) was introduced to overcome these challenges, delivering an exceptionally large ionic Seebeck coefficient (−3021 μV K^{-1}),

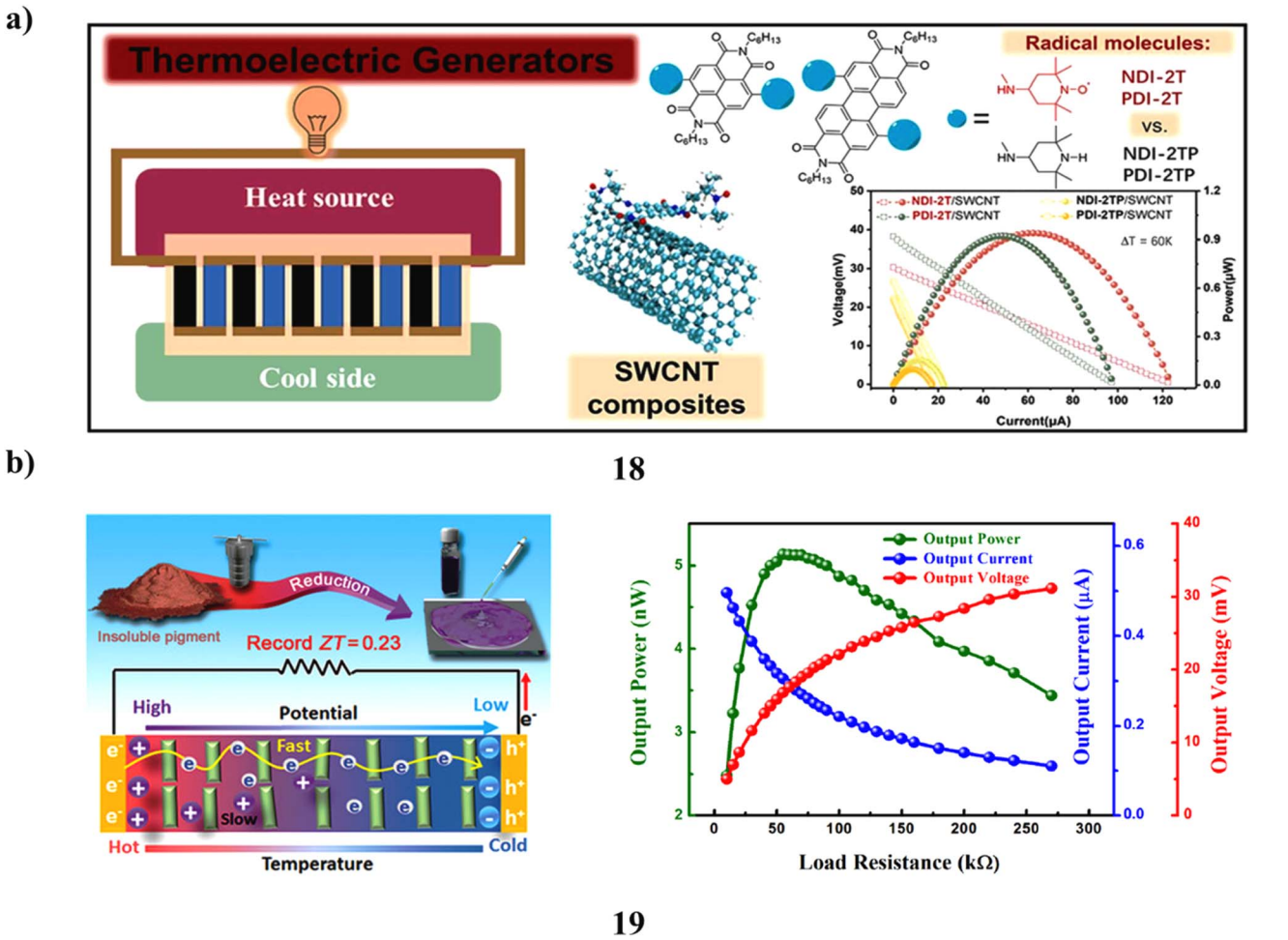

Fig. 10 (a) Radical-containing perylene composites boosting thermoelectric performance of SWCNT-based films (**18**) Reproduced from ref. 37 with permission from Elsevier Publisher, Copyright 2023. (b) High n-type thermoelectric performance in perylene bisimide *via* mixed ion-electron transport (**19**) Reproduced from ref. 38 with permission from Wiley-VCH Publisher, Copyright 2020.

electrical conductivity of 0.18 S cm^{-1}, and a high power factor of 165 μW m^{-1} K^{-2} with a *ZT* of 0.23 at room temperature. The enhanced performance arises from controlled ionic and electronic carrier transport, enabling stable single-leg thermoelectric generator operation (Fig. 10b).[38]

By combining the high electrical conductivity of single-walled carbon nanotubes (SWCNTs) with the large Seebeck coefficient of rylene diimide derivatives, an effective strategy was developed to fabricate high-performance n-type thermoelectric composites. The amino-substituted perylene diimide (PDINE) was incorporated into SWCNT networks to form n-type PDINE/SWCNT composites (**20**). The resulting materials exhibit significantly enhanced thermoelectric performance, achieving a maximum power factor of 112 ± 8 μW m^{-1} K^{-2}. Notably, a short doping time of only 0.5 h is sufficient to obtain optimal thermoelectric properties, enabling efficient and scalable processing. A thermoelectric module composed of five p–n junctions delivers an output power of 3.3 μW under a temperature gradient of 50 °C. Furthermore, the n-type composites demonstrate excellent air stability and thermal stability. Overall, this design strategy provides a promising route for the development of robust, high-performance n-type thermoelectric materials and devices (Fig. 11a).[39] Thermoactivated electrical conductivity was investigated in nanofibers fabricated from derivatives of perylene tetracarboxylic diimide (**21**, PTCDI) under both dark conditions and visible light illumination. The activation energies of nanofibers based on donor–acceptor (D–A) PTCDI derivatives were found to be higher than those of symmetric *n*-dodecyl-substituted PTCDI nanofibers. This difference arises from the strong sensitivity of thermally activated charge hopping to material disorder, which in D–A systems is dominated by charge-transfer interactions and dipole–dipole coupling between stacked molecules. Upon heating above the first phase transition temperature (~85 °C), a pronounced increase in activation energy was observed, attributed to enhanced polaronic effects at elevated temperatures. Additionally, visible light illumination significantly increases the charge carrier density in D–A PTCDI nanofibers. In agreement with established theoretical models, the increased carrier density leads to a reduction in activation energy due to an upward shift of the Fermi level toward the conduction band edge. These results highlight the interplay between molecular

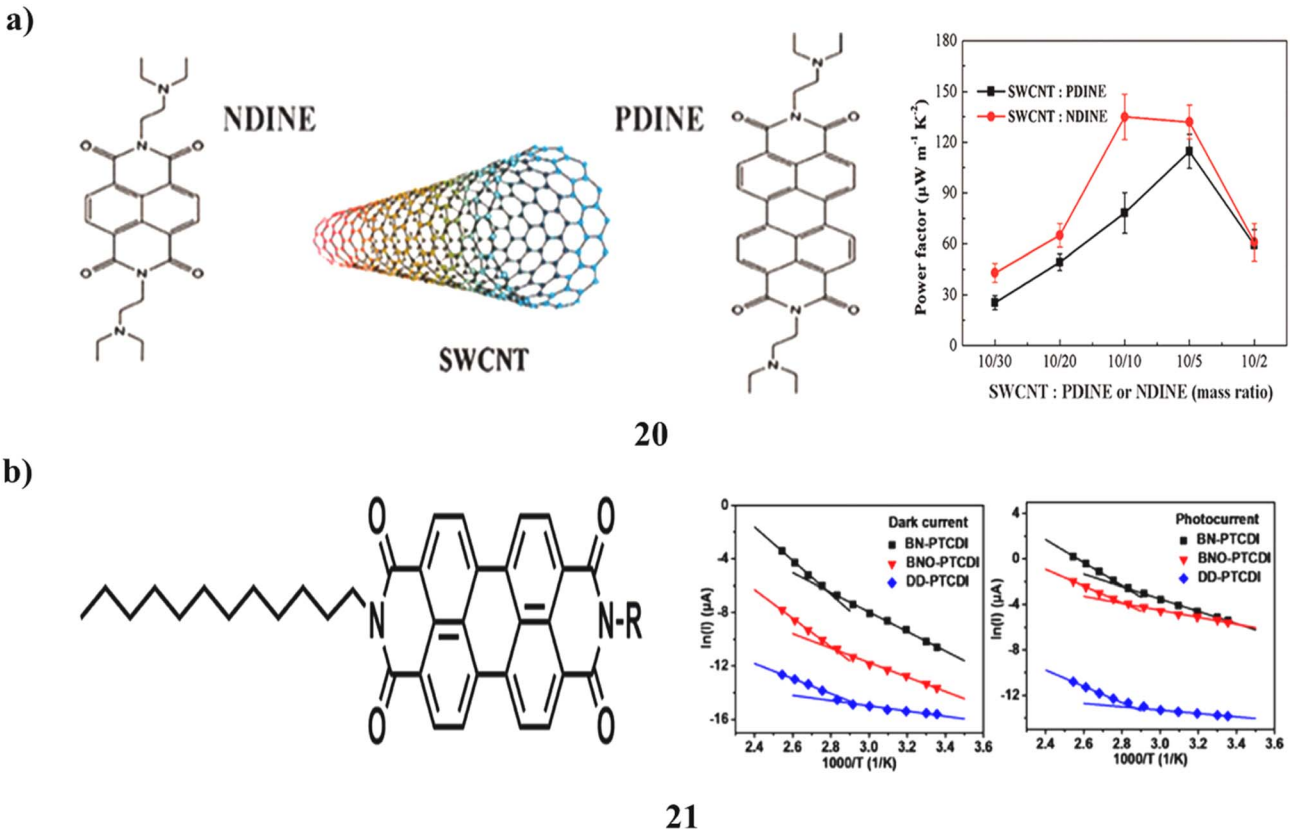

Fig. 11 (a) Amino-substituted perylene diimide/SWCNT composites for high-performance n-type thermoelectrics (**20**) Reproduced from ref. 39 with permission from ACS Publisher, Copyright 2017. (b) Thermoactivated electrical conductivity in perylene diimide nanofiber materials (**21**) Reproduced from ref. 40 with permission from ACS Publisher, Copyright 2017.

structure, thermal effects, and photoexcitation in governing charge transport in PTCDI nanofiber systems (Fig. 11b).[40]

Highly air- and temperature-stable, solution-processable n-type organic semiconductors based on a perylene diimide polymer (**22**) were successfully synthesized and characterized. When incorporated into field-effect transistor architectures exhibit pure n-type charge transport with the polymer achieving an electron mobility of up to 10^{-5} cm^2 V^{-1} s^{-1}. Despite its lower transistor mobility, the monomer displays excellent photoconductive behavior with photocurrent-to-dark-current ratios reaching up to 10^3. The distinct differences in transistor and photoconductor performance indicate that each material is suited for different device applications. Notably, both materials can be processed entirely in air and demonstrate remarkable air stability in their transport properties. Thermal annealing further enhances device performance, even at temperatures as

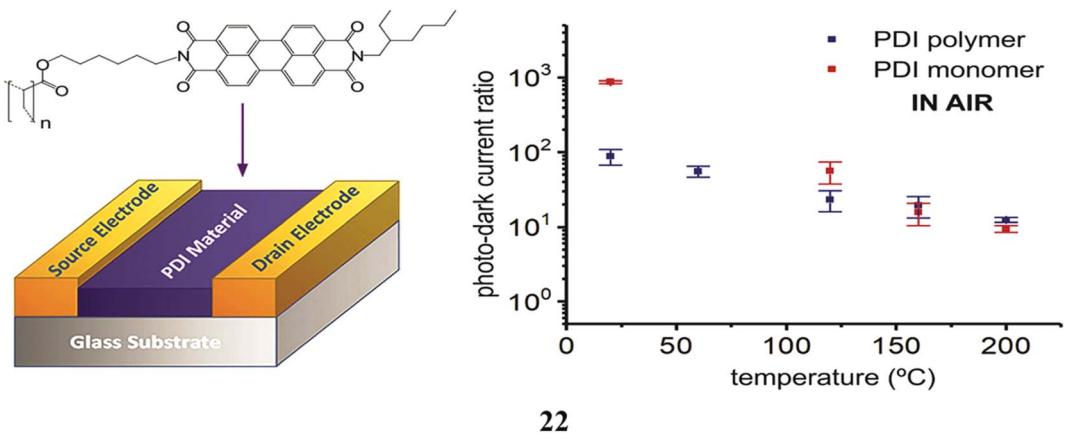

Fig. 12 Air- and temperature-stable perylene diimide-based n-type semiconductors for photoconductor and transistor applications (**22**) Reproduced from ref. 41 with permission from Elsevier Publisher, Copyright 2020.

high as 200 °C under ambient conditions. Such a combination of air-stable photoconductivity and charge transport is rarely observed in n-type organic semiconductors. Consequently, these materials hold strong potential for a broad range of optoelectronic and electronic applications (Fig. 12).[41]

Perylene-based thermoelectric materials operate on the Seebeck effect, where a temperature gradient induces charge carrier diffusion, and their planar π-conjugated perylene diimide (PDI) frameworks with deep LUMO levels make them particularly effective as air-stable n-type thermoelectrics. Their performance is characterized by enhanced electrical conductivity and moderate-to-high Seebeck coefficients achieved through molecular engineering, controlled n-doping, strong π–π stacking, and hybridization with carbon nanomaterials, leading to competitive power factors and emerging *ZT* values near room temperature. The detection mechanism relies on the generation of thermovoltage in response to small temperature differences, which is highly sensitive to carrier concentration, ionic–electronic coupling, and interfacial energy filtering effects within PDI-based films or composites. Selectivity arises from precise control over molecular structure, side-chain polarity, and dopant interactions, enabling preferential electron transport and, in some systems, selective response to thermal and humidity conditions through mixed ion–electron conduction. Key advantages include excellent chemical and thermal stability, well-defined molecular tunability, low thermal conductivity, solution processability, and strong potential for flexible and printable thermoelectric devices. However, disadvantages include relatively lower electrical conductivity compared to inorganic counterparts, dependence on precise doping control, sensitivity of performance to morphology and environmental conditions, and challenges in simultaneously maximizing conductivity and Seebeck coefficient, which still constrain large-scale practical applications.

4. Thermoelectric-based pyrrole

Polypyrrole/graphene nanosheet (PPy/GNs) composites (**23**) were prepared through a simple *in situ* polymerization approach to improve thermoelectric performance. Structural analyses (FTIR, Raman, SEM, and XRD) reveal strong π–π interactions between PPy and graphene, facilitating ordered chain growth and enhanced crystallinity. Increasing graphene content significantly improves both the Seebeck coefficient and

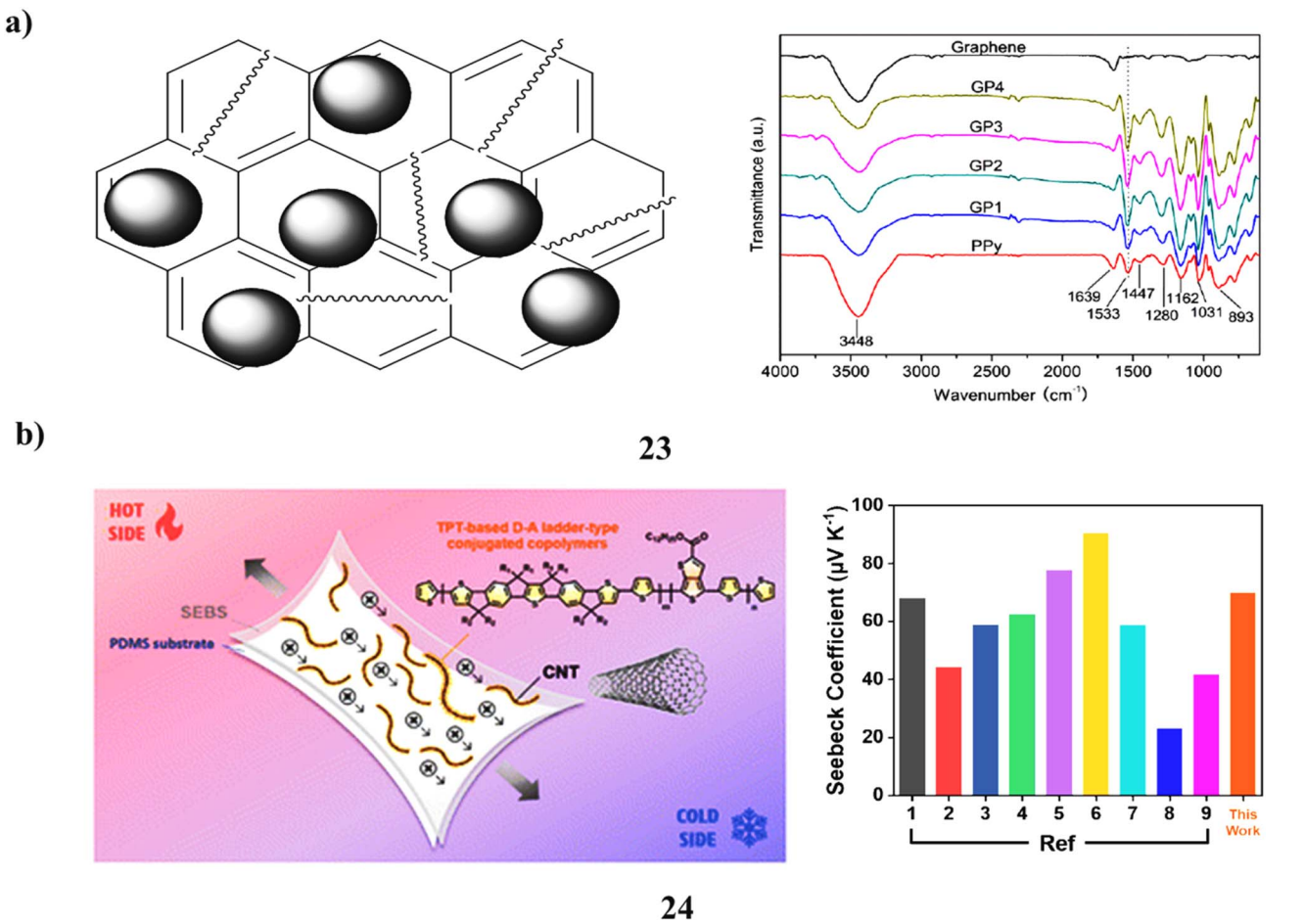

Fig. 13 (a) Polypyrrole/graphene nanosheet composites with enhanced thermoelectric properties (**23**) Reproduced from ref. 42 with permission from RSC Publisher, Copyright 2014. (b) Stretchable ladder-type conjugated polymer/CNT nanocomposites for thermoelectric films (**24**) Reproduced from ref. 43 with permission from RSC Publisher, Copyright 2024.

electrical conductivity, while thermal conductivity remains nearly constant. Consequently, the *ZT* value rises monotonically, reaching a maximum of 2.80×10^{-3} approximately 210 times higher than that of pristine PPy along with improved thermal stability (Fig. 13a).[42] Stretchable thermoelectric thin films are of significant interest for wearable electronics. Performance is often limited by increased resistance and reduced electrical conductivity under mechanical strain. The high-performance thermoelectric nanocomposites (**24**) were developed by blending thienyl–phenylene–thienylene–phenylene–thienyl (TPT) nonacyclic fused-ring conjugated polymers with single-walled carbon nanotubes (CNTs). To achieve effective CNT dispersion, ladder-type random TPT-based conjugated copolymers incorporating different acceptor units were investigated. Owing to its highly planar backbone, the TPT-TT polymer efficiently wraps around CNT surfaces, enabling uniform dispersion within the nanocomposite. As a result, the TPT-TT/CNT composite exhibits outstanding thermoelectric performance with a power factor of up to 678.8 μW m^{-1} K^{-2}. Furthermore, stretchable thermoelectric films were fabricated on poly(dimethylsiloxane) (PDMS) substrates by introducing varying amounts of styrene–ethylene–butylene–styrene (SEBS) elastomer. The optimized ternary TPT-TT/CNT/SEBS25 composite retains a power factor of 372.79 μW m^{-1} K^{-2}, corresponding to 73.2% of its initial value, even at 50% tensile strain. This work presents a simple and effective strategy for producing stretchable thermoelectric films with excellent performance under large mechanical deformation (Fig. 13b).[43]

Lamellar-structured polypyrrole doped with β-naphthalene sulfonic acid (β-NSA) (**25**) was synthesized using $FeCl_3$ as an oxidant, resulting in markedly improved thermoelectric performance compared to pristine PPy. The combined action of β-NSA and $FeCl_3$ directs the formation of an ordered lamellar morphology, facilitating enhanced charge transport and yielding a maximum *ZT* of 0.62×10^{-3} at 300 K about ten times higher than pure PPy. Moreover, the doped PPy exhibits improved thermal stability and mechanical strength, supporting its potential for practical applications (Fig. 14a).[44] Cationic polypyrrole nanoparticles (**26**, PPy:NPs) were synthesized in an aqueous medium to serve as templates for constructing flexible hierarchical architectures with enhanced thermoelectric performance. A distinctive multilayer structure was fabricated

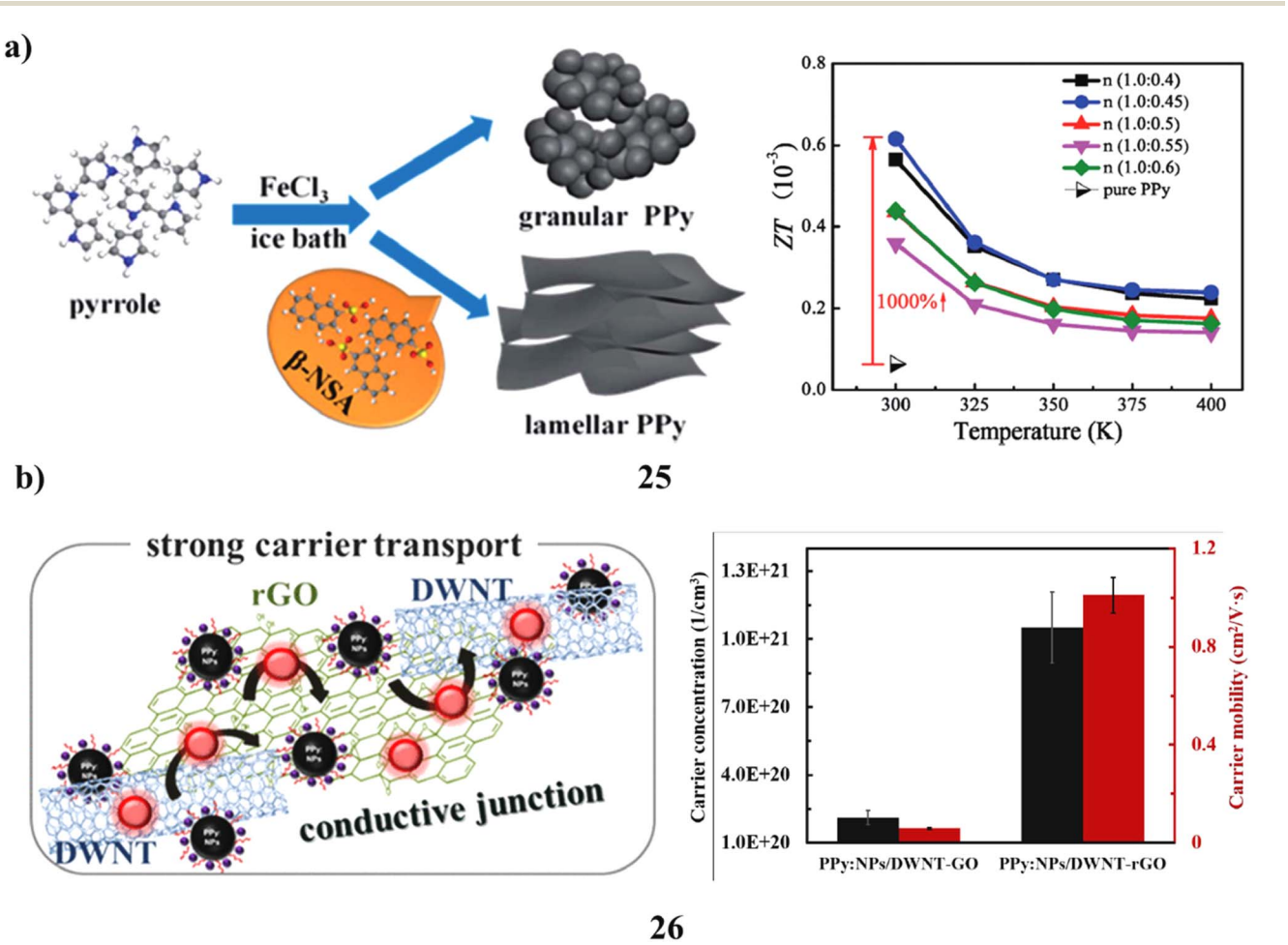

Fig. 14 (a) Lamellar polypyrrole doped with β-naphthalene sulfonic acid showing enhanced thermoelectric performance (**25**) Reproduced from ref. 44 with permission from RSC Publisher, Copyright 2023. (b) Polypyrrole-based multilayer nanoarchitectures with improved thermoelectric properties after thermal reduction (**26**) Reproduced from ref. 45 with permission from ACS Publisher, Copyright 2023.

through layer-by-layer assembly by alternately depositing positively charged PPy:NPs and negatively charged double-walled carbon nanotube-graphene oxide (DWNT-GO) suspensions. The resulting polymer/carbon composite, consisting of 16 PPy:NPs/DWNT-GO bilayers with a total thickness of approximately 2.45 μm, exhibited an electrical conductivity of 1.36 S cm^{-1} and a Seebeck coefficient of 84 μV K^{-1}, corresponding to a power factor of 0.96 μW m^{-1} K^{-2}. Subsequent thermal reduction at 175 °C for 90 min led to a dramatic enhancement in electrical conductivity (183.2 S cm^{-1}) and Seebeck coefficient (115 μV K^{-1}). As a result, an exceptional power factor of 242.2 μW m^{-1} K^{-2} was achieved, ranking among the highest reported for PPy-based organic thermoelectric materials. This outstanding performance is attributed to the formation of a highly ordered three-dimensional conjugated network after thermal reduction, which significantly facilitates charge carrier transport within the multilayered structure (Fig. 14b).[45]

The thermoelectric performance of nanocomposites composed of donor–acceptor random conjugated copolymers and single-walled carbon nanotubes (SWCNTs) was systematically investigated. By tuning the composition of the conjugated polymers through varying the ratio of diketopyrrolopyrrole (DPP) to isoindigo (IID), a series of random copolymers was designed to improve SWCNT dispersion into smaller bundles. Enhanced dispersion facilitates the formation of an interconnected conducting network, which is essential for optimizing thermoelectric performance. The influence of nanocomposite morphology on thermoelectric properties was comprehensively examined. The DPP95/SWCNT nanocomposite (**27**) exhibits the strongest polymer–CNT interactions, resulting in superior thermoelectric performance. A maximum power factor of 711.1 μW m^{-1} K^{-2} was achieved, arising from a high electrical conductivity of 1690 S cm^{-1} and a Seebeck coefficient of 64.8 μV K^{-1}. Furthermore, flexible thermoelectric generators fabricated using the DPP95/SWCNT film deliver a maximum power output of 20.4 μW m^{-2} under a temperature difference of 29.3 K. These results demonstrate that rational copolymer composition design combined with SWCNT incorporation is a promising strategy for harvesting low-grade waste heat in wearable thermoelectric applications (Fig. 15a).[46] The enhanced thermoelectric performance observed in these systems can be attributed to several key underlying mechanisms. First, molecular design and doping strategies play a crucial role in tuning the carrier concentration and optimizing the Fermi level, which directly influences both the Seebeck coefficient and electrical conductivity. Second, strong π–π stacking and improved molecular ordering facilitate

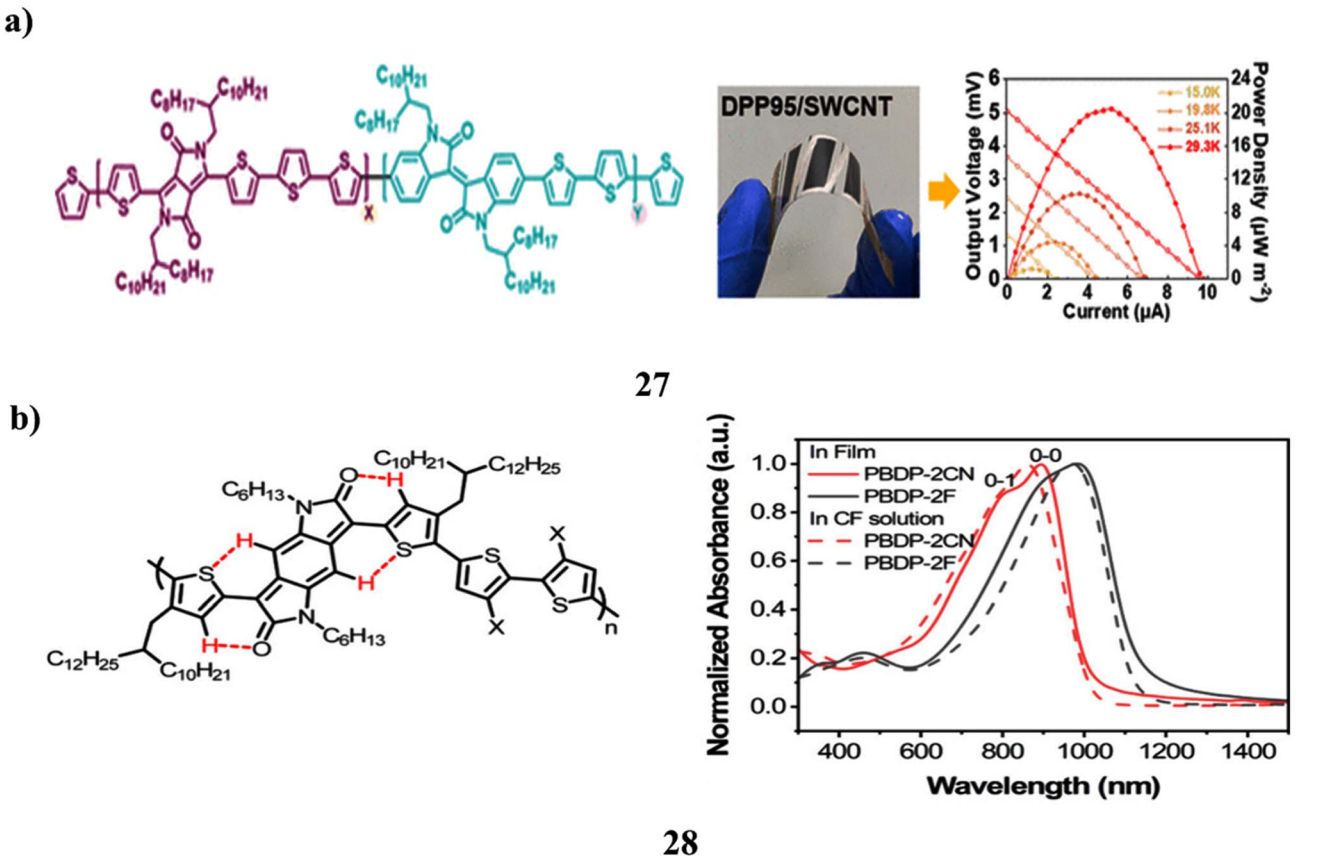

Fig. 15 (a) Diketopyrrolopyrrole/isoindigo copolymer–CNT nanocomposites with tunable thermoelectric performance (**27**) Reproduced from ref. 46 with permission from ACS Publisher, Copyright 2023. (b) Electron affinity-driven thermoelectric enhancement in quinoidal BDP polymer systems (**28**) Reproduced from ref. 47 with permission from ACS Publisher, Copyright 2024.

efficient charge transport by increasing carrier mobility. Third, interfacial effects in nanocomposites, such as energy filtering and carrier scattering at heterojunctions, selectively enhance high-energy carrier transport, leading to improved thermopower. Additionally, phonon scattering at interfaces and structural boundaries reduces thermal conductivity, thereby contributing to an overall increase in the thermoelectric figure of merit. These synergistic effects highlight the importance of a mechanistic approach in the rational design of high-performance organic thermoelectric materials. Efficient charge transport and high doping efficiency are critical for achieving high-performance organic thermoelectric materials, yet suitable electron-deficient polymer building blocks remain scarce. In this study, the quinoidal unit benzodipyrrolidone (BDP) is introduced into organic thermoelectrics for the first time. The n-doping behavior and thermoelectric properties of two BDP-based n-type polymers (**28**) were systematically investigated. It exhibits a lower LUMO energy level (−4.13 eV) reflecting a 0.11 eV enhancement in electron affinity. This higher electron affinity enables more efficient n-doping, leading to superior thermoelectric performance. Raman spectroscopy further reveals the excellent structural stability of quinoidal-based polymers upon doping, with minimal changes in vibrational modes. These results establish BDP as a promising building block for organic thermoelectrics and provide valuable molecular design guidelines for high-performance n-type polymer systems (Fig. 15b).[47]

Ionically interconnected polypyrrole (**29**, PPy) films were synthesized *via* two-monomer-connected-precursor polymerization using different diacid linkers to modulate crystalline morphology and charge transport. The PPy film incorporating 1,5-naphthalenedisulfonic acid (PPy-Nap) exhibits significantly higher electrical conductivity (~78 S cm^{-1}) than the linker-free PPy-ref (6.7 S cm^{-1}), along with ~5-fold higher carrier mobility. Structural analysis by 2D grazing-incidence X-ray scattering correlates improved crystallinity with reduced transport barriers in PPy-Nap. Despite similar Seebeck coefficients (5–8 μV K^{-1}) due to comparable doping levels, PPy-Nap achieves a higher power factor (0.21 *vs.* 0.043 μW m^{-1} K^{-2}). These results demonstrate that optimizing crystalline order and carrier mobility can overcome the conductivity-Seebeck trade-off and enhance thermoelectric performance (Fig. 16a).[48] Polypyrrole/

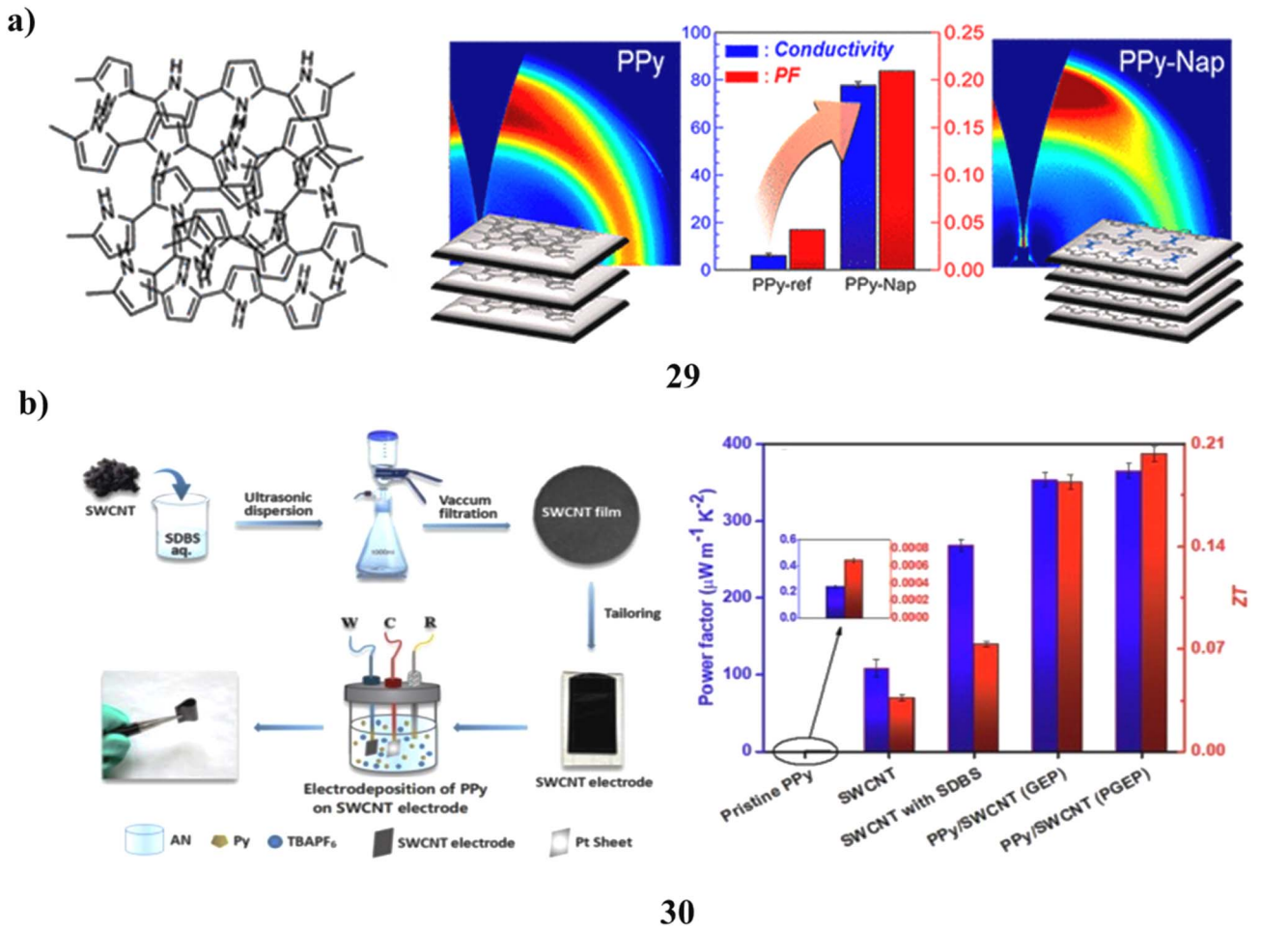

Fig. 16 (a) Higher thermoelectric efficiency achieved through improved chain ordering in cross-linked polypyrrole (**29**) Reproduced from ref. 48 with permission from ACS Publisher, Copyright 2020. (b) *In situ* pulse-electropolymerized polypyrrole/SWCNT composites for high thermoelectric performance (**30**). Reproduced from ref. 49 with permission from Elsevier Publisher, Copyright 2022.

SWCNT composites (**30**) were fabricated *via in situ* electropolymerization, where pulse galvanostatic electropolymerization optimized the interfacial structure and enhanced charge transport. This interface engineering strategy improved energy filtering effects, leading to excellent thermoelectric performance. The optimized composite achieved a high power factor of 365.2 μW m^{-1} K^{-2} and a *ZT* of 0.203 at room temperature, demonstrating the effectiveness of pulse electropolymerization for advanced TE materials (Fig. 16b).[49]

The electrical conductivity of conducting polymers is highly dependent on polymer chain alignment, with enhanced conjugation achieved through a fully aligned backbone. To improve chain alignment, pyrrole units were incorporated into the polyaniline (PANi) backbone. A nanostructured poly(aniline-*co*-pyrrole) random copolymer (**31**, PANiPy) was successfully synthesized *via* a sustainable, agitation-free method. FTIR, Raman, and XPS analyses confirmed strong interactions between aniline and pyrrole units. Single-walled carbon nanotubes (SWCNTs) were introduced to enhance membrane formation and composite processability. SEM studies revealed a nanostructured morphology with PANiPy well dispersed within SWCNT bundles. The composite exhibited a self-assembled layered structure and achieved a high power factor of 98.5 μW m^{-1} K^{-2}. These results demonstrate that pyrrole incorporation effectively enhances PANi chain alignment and thermoelectric performance through a sustainable synthesis route (Fig. 17a).[50] Waste plastic-derived reduced graphene oxide synthesized using copper turnings as a catalytic template exhibited superior thermoelectric performance when combined with polypyrrole. The conversion of waste plastic into graphene nanosheets provides a sustainable route for effective plastic waste management. Subsequent transformation into conducting graphene nanosheets enables their application in energy conversion materials. Intercalation of graphene nanosheets with polypyrrole led to the formation of a PPy/GNs nanocomposite (**32**) demonstrating the potential of pyrrole-based composites for thermoelectric devices. Polypyrrole's intrinsic electrical conductivity and thermal stability facilitate efficient charge transport and reliable device operation. The composite displayed semiconducting behavior with extremely low resistivity, resulting in high electrical conductivity. Enhanced Seebeck coefficient and figure of merit (*ZT*) values confirmed the

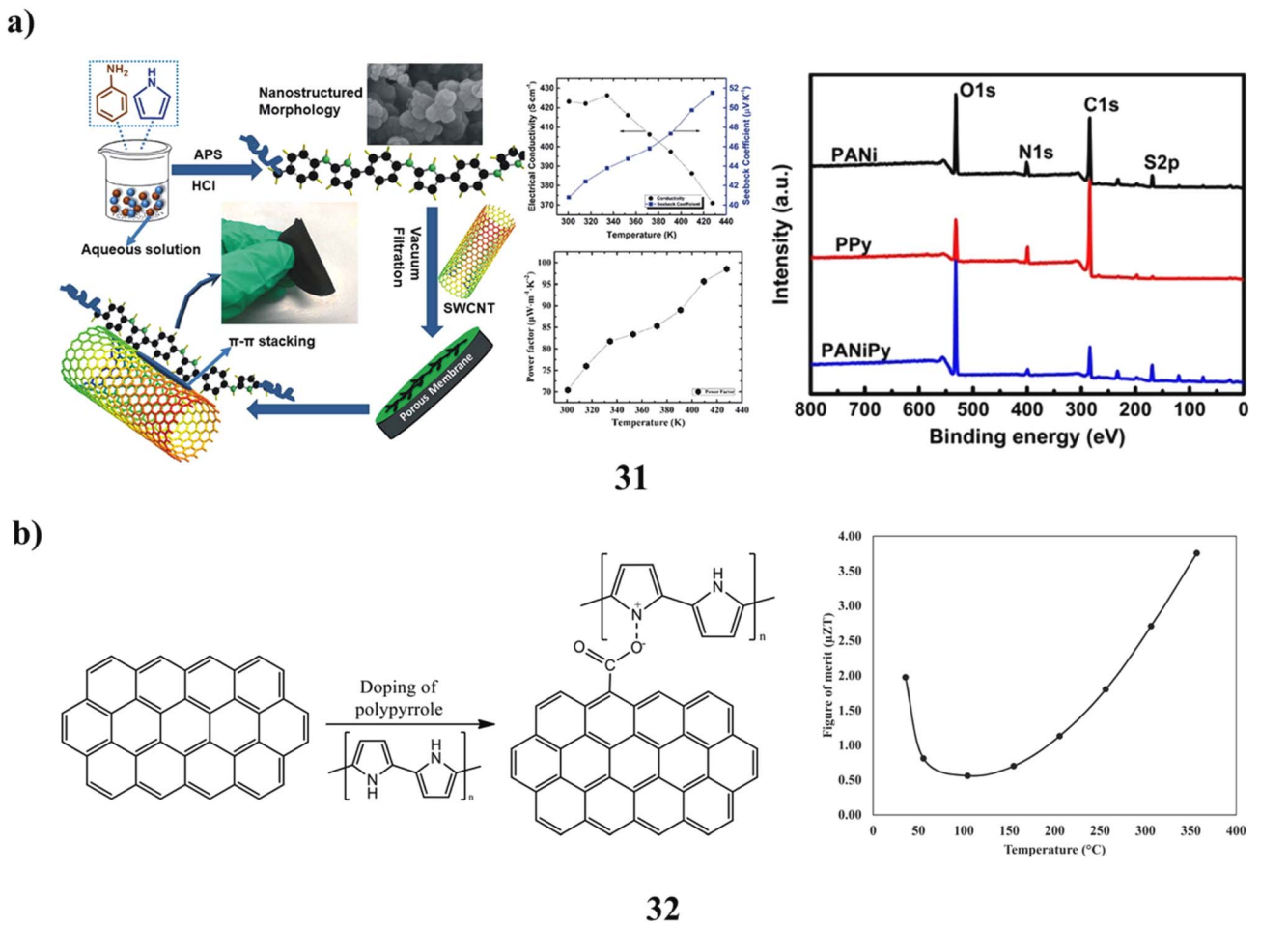

Fig. 17 (a) Pyrrole-modified polyaniline/CNT composites with improved thermoelectric performance (**31**) Reproduced from ref. 50 with permission from Elsevier Publisher, Copyright 2019. (b) Plastic waste-derived graphene/polypyrrole nanocomposites for thermoelectric applications (**32**) Reproduced from ref. 51 with permission from Elsevier Publisher, Copyright 2025.

strong thermoelectric response of the nanocomposite. Overall, this work highlights a sustainable strategy for producing graphene-based thermoelectric materials from plastic waste (Fig. 17b).[51]

The thermoelectric properties of a diketopyrrolopyrrole-based semiconductor (**33**, PDPP3T) were investigated using a controlled iron(III) chloride doping process. The doping level of PDPP3T films was linearly tuned by adjusting the dopant concentration. Owing to its high intrinsic Seebeck coefficient, PDPP3T exhibited excellent power factors exceeding 200 μW m^{-1} K^{-2} over a wide doping range of 3–8 mM. A maximum power factor of 276 μW m^{-1} K^{-2} was achieved, significantly surpassing that of poly(3-hexylthiophene). The high charge-carrier mobility of PDPP3T contributed to enhanced electrical conductivity, while low dopant volume helped preserve a high Seebeck coefficient. Furthermore, the low-bandgap nature of PDPP3T shifted its optical absorption into the near-infrared region and rendered the films more colorless upon doping. This feature is advantageous for transparent electronic applications. Overall, the results highlight the importance of low-bandgap, high-mobility polymers and precise doping control in achieving high thermoelectric performance (Fig. 18a).[52] Highly conductive PPy/SWCNT composite films (**34**) were fabricated *via* temperature-controlled chemical interfacial polymerization, yielding smooth, compact morphologies with extended conjugation and ordered structures. The composites exhibited high electrical conductivity (~500 S cm^{-1}), while SWCNT incorporation significantly enhanced the Seebeck coefficient through synergistic and energy-filtering effects. As a result, a power factor of 37.6 ± 2.3 μW m^{-1} K^{-2} was achieved nearly three orders of magnitude higher than conventional PPy highlighting interfacial polymerization as an effective route for advanced thermoelectric nanocomposites (Fig. 18b).[53]

Pyrrole-based thermoelectric materials, mainly represented by polypyrrole (PPy) and its composites, operate on the Seebeck principle in which a temperature gradient drives charge carrier diffusion along the conjugated polymer backbone, generating a measurable thermovoltage. Their thermoelectric performance is governed by doping level, chain alignment, and interfacial engineering, with enhanced electrical conductivity and Seebeck coefficient achieved through acid doping, nanostructuring, and hybridization with graphene or carbon nanotubes, resulting in moderate power factors and low thermal conductivity. The detection mechanism relies on changes in voltage output in response to temperature differences, which are highly sensitive to carrier concentration, polymer morphology, and interfacial charge transport pathways. Selectivity is primarily structural and thermal rather than chemical, arising from controlled doping, ordered lamellar or multilayer architectures, and energy-filtering effects at polymer–carbon interfaces that favor specific charge carriers. Key advantages include low cost, facile synthesis, mechanical flexibility, environmental friendliness,

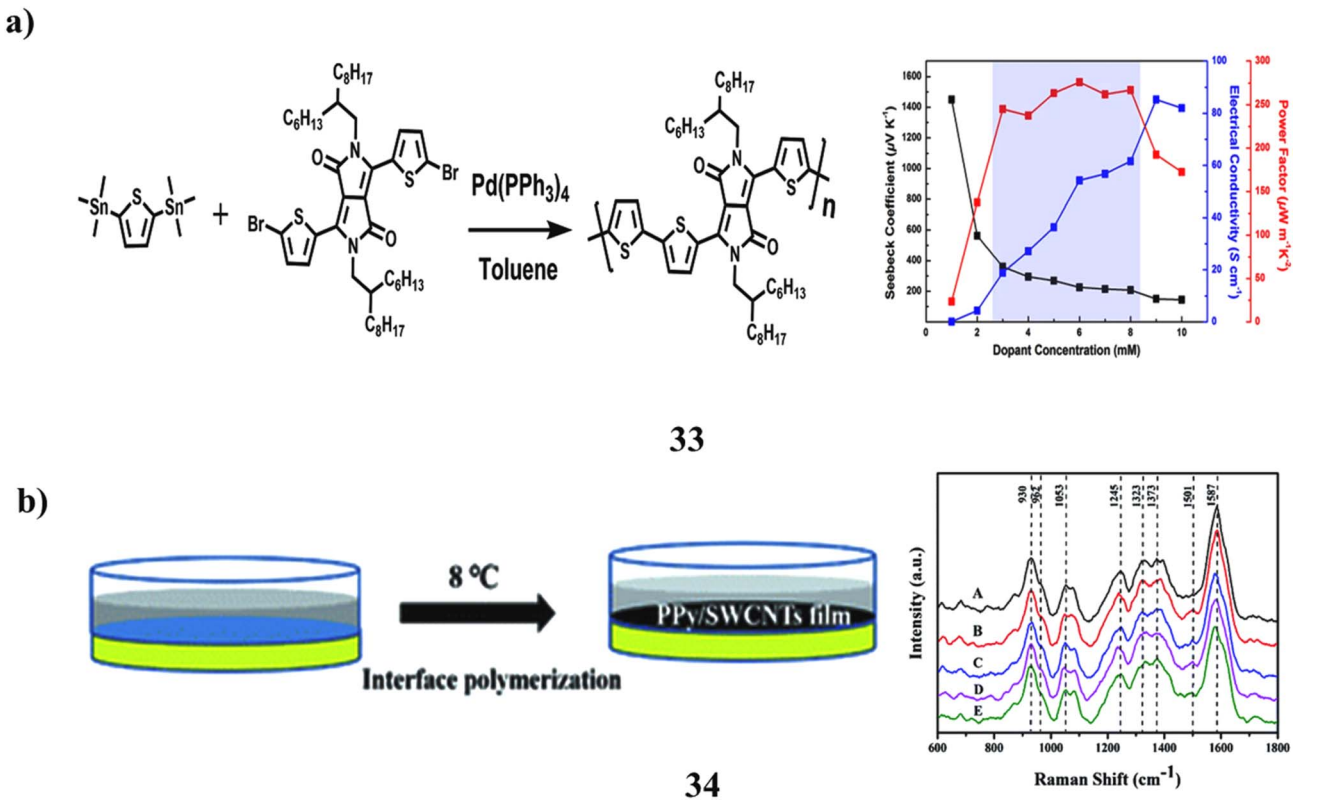

Fig. 18 (a) Doping-controlled thermoelectric enhancement in low-bandgap conjugated polymers (**33**) Reproduced from ref. 52 with permission from Nature Publisher, Copyright 2017. (b) High-performance polypyrrole/SWCNT composite films for organic thermoelectrics (**34**) Reproduced from ref. 53 with permission from RSC Publisher, Copyright 2021.

solution processability, and compatibility with flexible and wearable thermoelectric devices. However, disadvantages include intrinsically lower carrier mobility than inorganic materials, limited long-term stability under high temperature or humidity, performance variability due to structural disorder, and difficulty in simultaneously optimizing electrical conductivity and Seebeck coefficient, which restricts overall efficiency.

5. Thermoelectric-based thiophene

The organometallic nickel complex incorporating thieno[3,2-*b*] thiophene units (**35**) was rationally designed and synthesized. Composite films based on the nickel complex and poly(-vinylidene difluoride), fabricated *via* a simple solution-processing method under ambient conditions, exhibit exceptionally high n-type electrical conductivity exceeding 200 S cm^{-1}. Notably, the resulting n-type composite films display excellent air-stable thermoelectric power factors. Grazing-incidence wide-angle X-ray diffraction analysis reveals that incorporation of the thieno[3,2-*b*]thiophene core significantly influences molecular orientation within the composite films, contributing to the enhanced charge transport properties (Fig. 19a).[54] Inorganic–organic interfaces offer a promising route to achieve the strong electrical and thermal asymmetries required for efficient thermoelectric performance. The transport properties of such interfaces were investigated at the molecular scale using scanning tunneling microscope break-junction measurements, theoretical analysis, and a newly synthesized series of disubstituted thiophene derivatives (**36**). These molecules systematically vary in alkylthio linker length and the number of thiophene units, enabling controlled tuning of electronic resonances within the junctions. The Seebeck coefficient decreases with increasing alkyl chain length, whereas oligothiophene junctions exhibit an increase in the Seebeck coefficient with molecular length, reaching values of 7–15 μV K^{-1}. A minimal tight-binding model incorporating a gateway state associated with the S–Au bond successfully captures and explains both trends. This study highlights S–Au gateway states as critical and tunable features of junction electronic structure for enhancing the thermoelectric power factor at organic–inorganic interfaces (Fig. 19b).[55]

Sulfur–nickel (S–Ni) complex polymers (**37**) possess a planar, tetra-coordinated architecture in which a central nickel atom is surrounded by four sulfur atoms, imparting stable electrical and thermal properties without the need for external dopants. To enhance the solubility of the ligand precursors, a cyanoethyl-substitution strategy was employed, enabling the successful synthesis of three new S–Ni complex polymers: NiTTFtt, incorporating tetrathiafulvalene (TTF) donor units; NiDMTtt, featuring a thiophene-inserted TTF backbone; and NiDMT2tt,

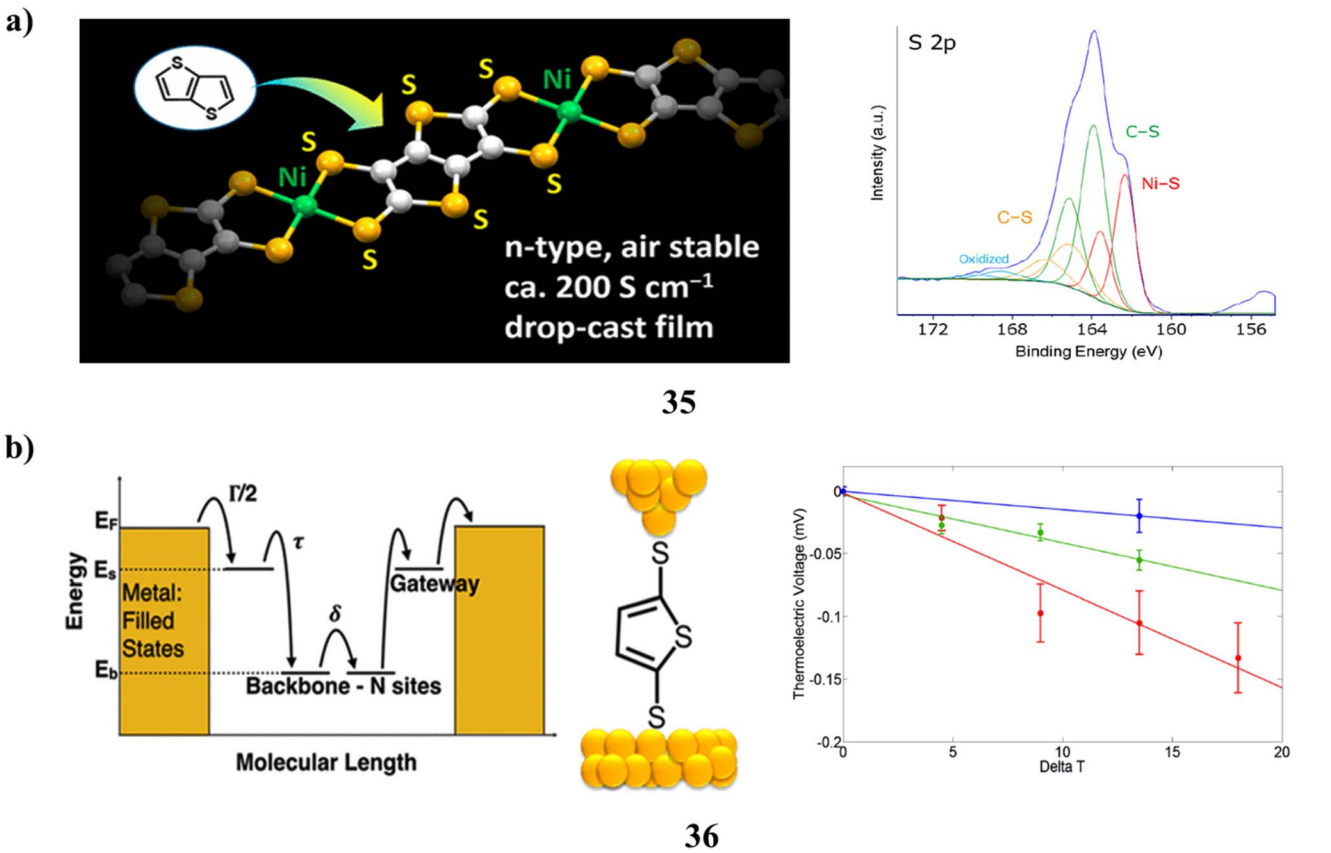

Fig. 19 (a) n-Type nickel coordination complex with thieno[3,2-*b*]thiophene units showing high thermoelectric performance (**35**) Reproduced from ref. 54 with permission from ACS Publisher, Copyright 2022. (b) Tunable thermoelectric properties of thiophene-derived single-molecule junctions (**36**) Reproduced from ref. 55 with permission from ACS Publisher, Copyright 2014.

containing thienothiophene units within the TTF backbone. The latter two polymers adopt bent conformations at the alkene moieties. Further compositional tuning was achieved by introducing alkali metal counterions (Na^+ and K^+) and partially incorporating Ni^{2+} ions, yielding a total of six distinct S–Ni complex polymers. These materials were processed into thermoelectric pellets for performance evaluation. Among them, NiTTFFtt exhibits the highest electrical conductivity (575.90 S cm^{-1}), whereas NiDMTtt and NiDMT2tt show lower conductivities but higher Seebeck coefficients, reaching up to 37.09 μV K^{-1}. Systematic investigation of alkali metal ion doping effects reveals an effective strategy for optimizing the thermoelectric properties of S–Ni complex polymers, providing important insights into the molecular design and functional tuning of metallopolymers for high-performance thermoelectric applications (Fig. 20a).[56] The conductive thiophene-based polymers have attracted considerable interest for organic electronic applications, including electrochromic and thermoelectric materials; however, their practical development is often limited by poor electron transport and insufficient long-term stability. To address these challenges, a molecular engineering strategy was implemented by functionalizing thiophene-based polymers (**38**) with oligo(ethylene glycol) or alkyl side chains, leading to the synthesis of a series of poly(3,4-ethylenedioxy bithiophene)s (PEDTs) with tunable electrochromic and thermoelectric properties. Incorporation of electronically active alkyl substituents on the thiophene ring significantly enhances electrical conductivity while maintaining an almost constant Seebeck coefficient, resulting in an order-of-magnitude improvement in the thermoelectric power factor. In addition, the functionalized PEDTs exhibit markedly improved electrochromic performance, including higher optical contrast, enhanced coloration efficiency, and improved operational stability with multicolor switching between neutral and oxidized states. This work demonstrates that side-chain functionalization provides an effective strategy for simultaneously optimizing the electrochromic and thermoelectric properties of thiophene-based polymer materials (Fig. 20b).[57]

n-Type polythiophenes are promising polymer thermoelectric materials due to their simple structures and scalable synthesis, yet their performance is often limited by twisted backbones and poor π-stacking arising from dense electron-withdrawing substituents. Thiazole-inserted polythiophene derivatives (**39**, PTTz), based on thieno[3,4-*c*]pyrrole-4,6-dione and thiophene-3,4-dicarbonitrile units, were designed to address these limitations. Thiazole incorporation significantly

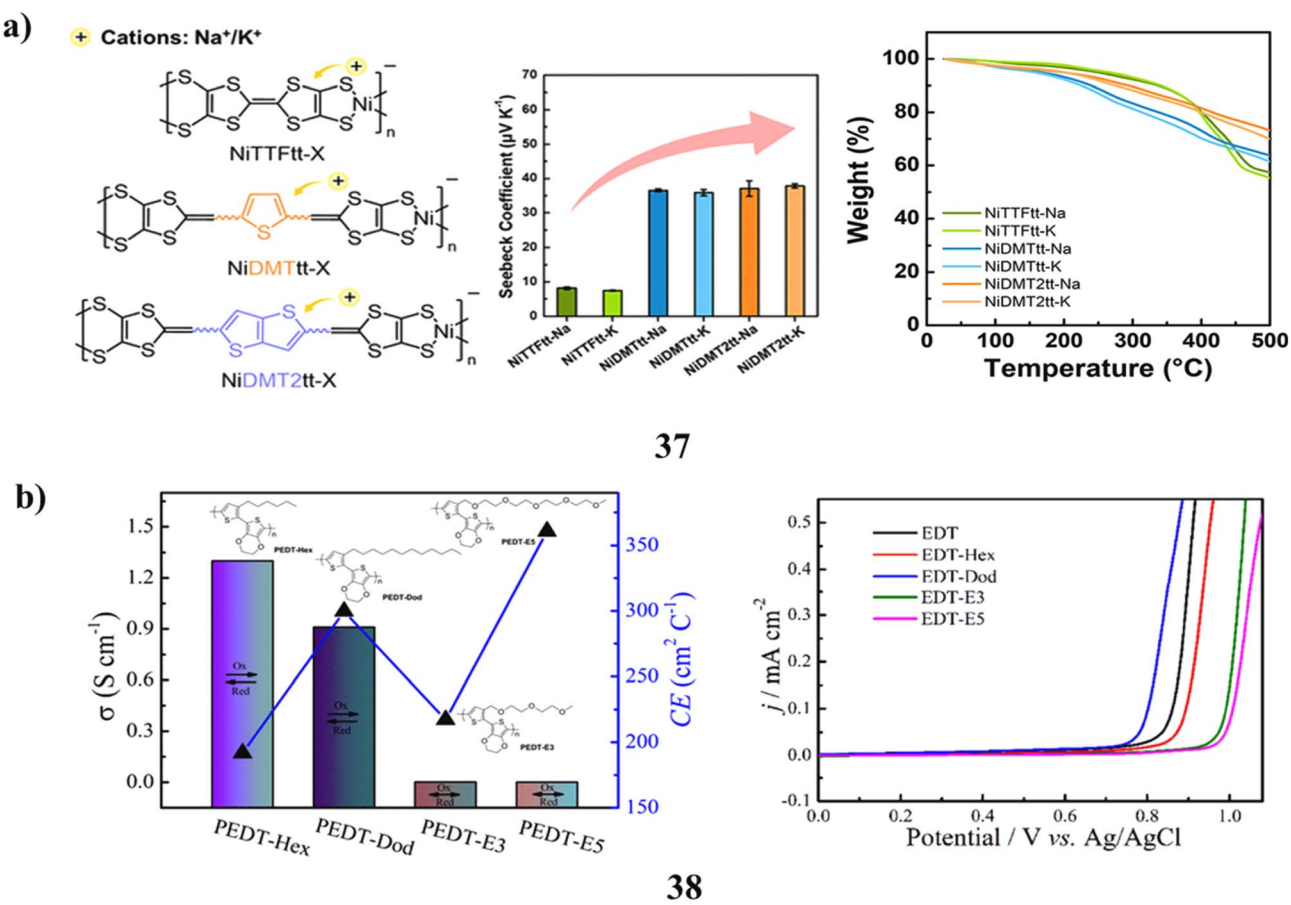

Fig. 20 (a) Sulfur–nickel tetrathiolate metallopolymers with enhanced thermoelectric properties (**37**) Reproduced from ref. 56 with permission from ACS Publisher, Copyright 2025. (b) Functionalized poly(3,4-ethylenedioxybithiophene) films enable tunable electrochromic and thermoelectric performance (**38**) Reproduced from ref. 57 with permission from ACS Publisher, Copyright 2017.

planarizes the polymer backbone while maintaining deep LUMO levels, leading to enhanced π-stacking, higher electron mobility, and efficient n-doping. Consequently, the polymers exhibit superior thermoelectric performance, achieving an electrical conductivity of 50.3 S cm^{-1} and a power factor of 23.8 μW m^{-1} K^{-2}. This work underscores the critical role of thiazole units in the molecular design of high-performance n-type polymer thermoelectrics (Fig. 21a).[58] Manipulating the connectivity between external electrodes and the central ring of carbon-based molecules in single-molecule junctions provides an effective strategy for tuning thermoelectric properties. The connectivity-dependent thermoelectric behavior of thiophene–diketopyrrolopyrrole (**40**, DPP) derivatives was investigated using density functional theory, tight-binding modeling, and quantum transport calculations. Electrical conductance is found to depend strongly on the connectivity of the thiophene units to the DPP core. For connectivities exhibiting constructive quantum interference (CQI), different isomers generated by thiophene ring rotation show identical conductance, whereas destructive quantum interference (DQI) connectivities display pronounced conductance variations. Notably, DQI configurations yield significantly enhanced Seebeck coefficients in the range of 500–700 μV K^{-1}. Upon including phonon thermal conductance, the resulting thermoelectric figure of merit (*ZT*) for CQI molecules reaches ~1.5 at room temperature and increases to ~2 at 400 K. Furthermore, doping with tetracyanoquinodimethane induces charge transfer with the DPP core, enabling reversal of the Seebeck coefficient sign (Fig. 21b).[59]

State-of-the-art p-type organic thermoelectrics are largely based on thiophene-derived conjugated polymers. However, innovative molecular design and exploration of alternative backbones are crucial for achieving higher performance and deeper insight into donor–acceptor systems. In this context, two novel electroactive oligomeric materials (**41**) were designed and synthesized using a terthiophene donor unit coupled with a strongly electron-withdrawing naphthalimide acceptor. These molecular assemblies were polymerized *via* palladium-catalyzed cross-coupling reactions employing different linkers. The resulting materials exhibit extended optical absorption up to 1000 nm and enhanced hole field-effect mobilities reaching 1.8 × 10^{-3} cm^2 V^{-1} s^{-1} (Fig. 22a).[60] Achieving high electrical conductivity in n-type polymers is difficult because efficient electron injection and transport require deep LUMO energy levels and stable doping. To overcome this, electron-deficient bithiazole (BTz) units were incorporated into the BTPD

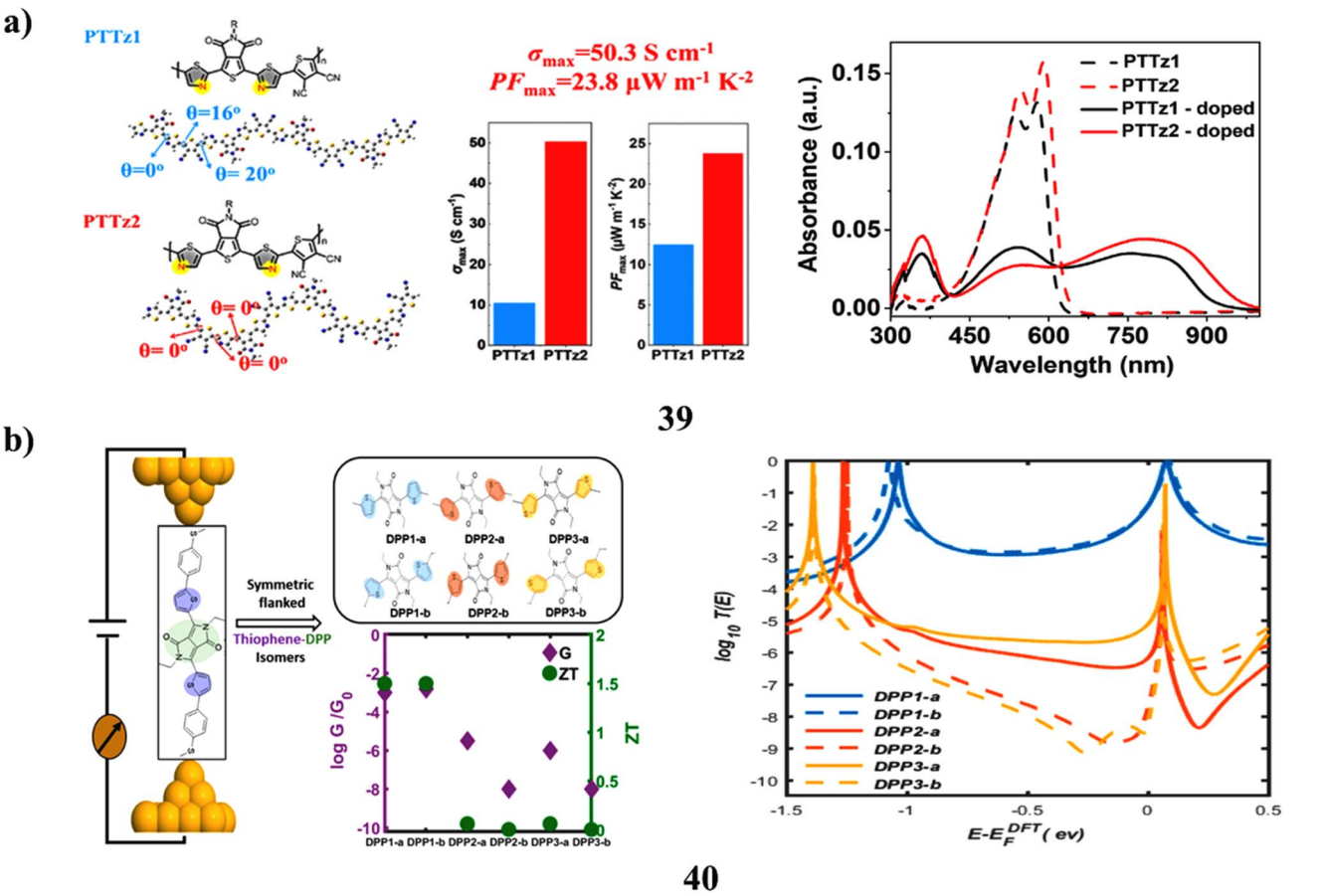

Fig. 21 (a) Thiazole-inserted n-type polythiophene derivatives with improved thermoelectric performance (**39**) Reproduced from ref. 58 with permission from ACS Publisher, Copyright 2024. (b) Quantum-interference-enhanced thermoelectric behavior in thiophene–diketopyrrolopyrrole molecular junctions (**40**) Reproduced from ref. 59 with permission from ACS Publisher, Copyright 2021.

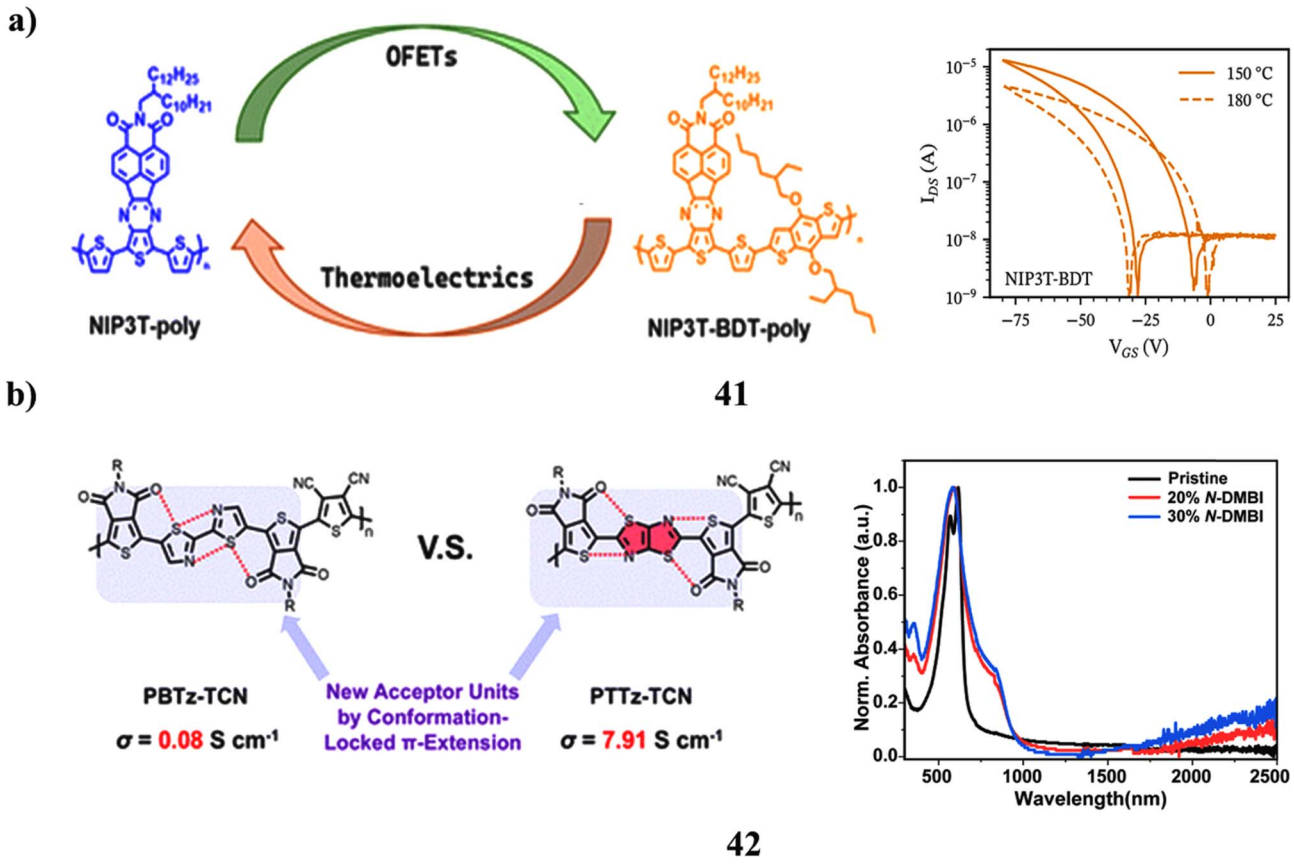

Fig. 22 (a) Low-bandgap oligothiophene–naphthalimide semiconductors enable efficient thermoelectric performance through enhanced charge transport and tunable electronic properties (**41**) Reproduced from ref. 60 with permission from RSC Publisher, Copyright 2025. (b) Conformation-locked n-type polymer semiconductors for organic thermoelectrics (**42**) Reproduced from ref. 61 with permission from RSC Publisher, Copyright 2025.

framework (**42**) to create conformation-locked building blocks with enhanced planarity and stronger electron affinity. The resulting polymers exhibited ultralow LUMO levels (−4.21 eV), facilitating effective n-doping with N-DMBI. Among them, PTTz-TCN showed significantly improved electrical conductivity (7.91 S cm^{-1}) and a higher power factor compared to reference polymers, demonstrating that extending acceptor cores with electron-withdrawing π-bridges and conformational locking effectively enhances electron transport and thermoelectric performance (Fig. 22b).[61]

The conjugated polymer (**43**, PTbTTVT) was synthesized through copolymerization of thieno[3,4-*b*]thiophene derivatives with a TVT linker (1,2-bis(3-tetradecylthiophen-2-yl)ethene). It exhibits favorable molecular orientation and enhanced charge mobility, whereas fluorine substitution induces disordered stacking and reduced hole mobility in PTbTTVT-F. Despite these structural differences, both polymers demonstrate good thermoelectric performance, achieving maximum power factors exceeding 35 μW m^{-1} K^{-2}. Notably, comparable or improved power factors can be obtained through appropriate dopant selection. These findings suggest that polymers with less ordered stacking may better tolerate dopant-induced disruption, and that leveraging amorphous materials with high intrinsic mobility represents a promising strategy for developing high-performance organic thermoelectric materials (Fig. 23a).[62] Organic materials have emerged as attractive candidates for thermoelectric applications due to their inherent advantages over inorganic counterparts; however, small-molecule organic semiconductors remain underexplored because of the difficulty in achieving highly conductive films. Progress in this area requires the development of new materials and a deeper understanding of structure–property relationships. In this study, the thermoelectric properties of two thiophene-based small molecules (**44**, OT), differing only in end-group substitution with varying acceptor strengths, were investigated. The difference in acceptor strength leads to distinct self-assembled morphologies and markedly different thermoelectric performances upon $FeCl_3$ doping. One molecule exhibits high electrical conductivity and a power factor of 52.0 μW m^{-1} K^{-2}, whereas the other shows significantly lower conductivity and a power factor of 1.6 μW m^{-1} K^{-2} under identical conditions. The superior performance arises from the weaker end-group acceptor strength, which enables higher doping efficiency, a lower-lying HOMO energy level, and an increased density of states near the HOMO after doping. Preservation of the self-assembled structure upon doping further

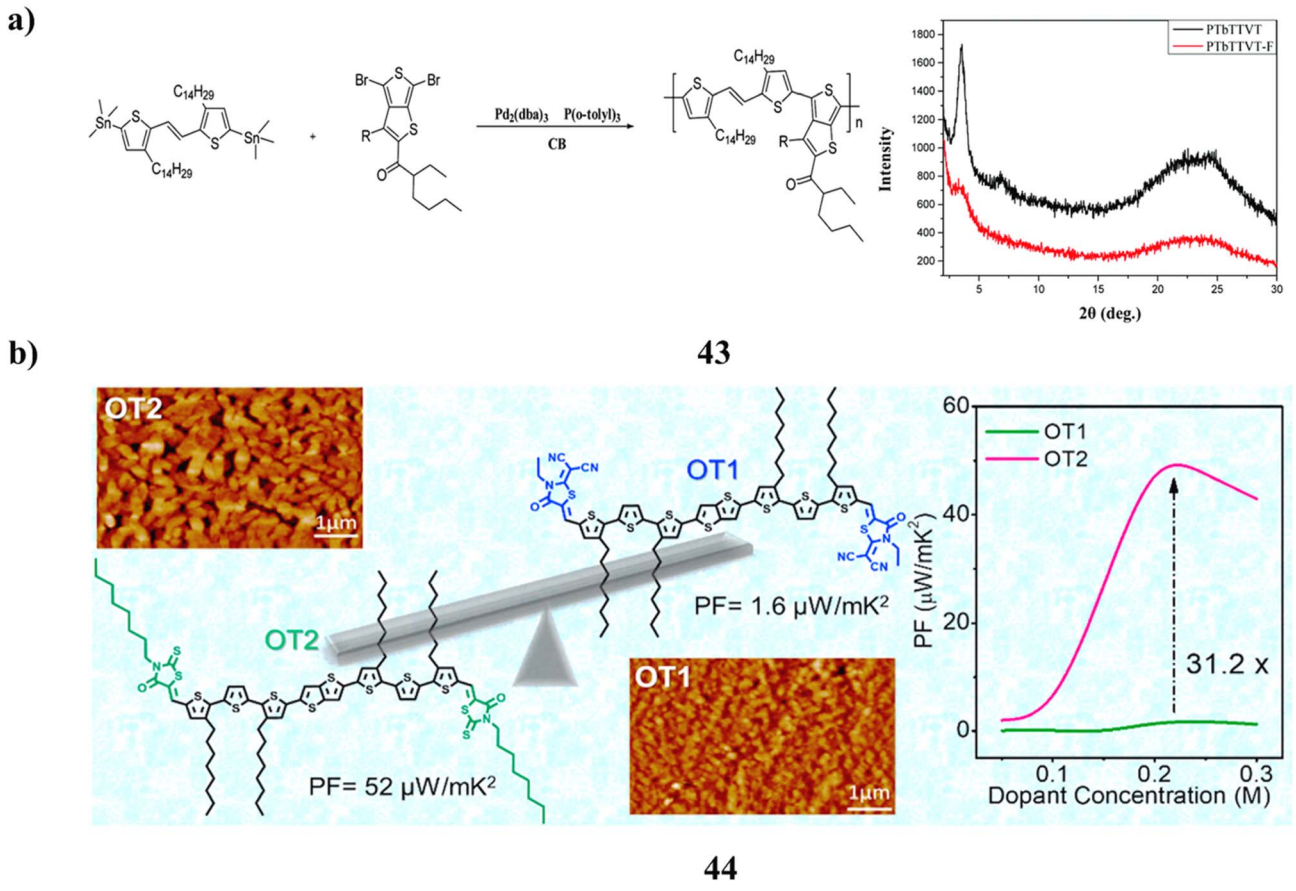

Fig. 23 (a) Doped thieno[3,4-*b*]thiophene-based copolymers for p-type thermoelectrics (**43**) Reproduced from ref. 62 with permission from RSC Publisher, Copyright 2021. (b) Structure-dependent thermoelectric properties of self-assembled thiophene derivatives (**44**) Reproduced from ref. 63 with permission from Elsevier Publisher, Copyright 2023.

contributes to efficient charge transport. These results highlight the critical role of molecular engineering in the design of high-performance organic thermoelectric materials (Fig. 23b).[63]

Carbon nanotube-based organic composites represent a promising platform for next-generation thermoelectric materials, where performance optimization relies on the rational design of organic molecules with strong nanotube interactions. In this work, a series of thiophenecarboxylates (**45**) incorporating electron-donating TEMPO radicals was designed, synthesized, and hybridized with single-walled carbon nanotubes to form thermoelectric composites. The molecules feature a donor–acceptor–donor architecture comprising electron-donating thiophene units and electron-withdrawing carbonate groups. Incorporation of TEMPO radicals enhances molecule–nanotube interactions, while the electronic effects of the carbonate and thiophene groups modulate doping behavior and charge-transfer efficiency. These results demonstrate the effectiveness of molecular engineering *via* electronic structure control for developing high-performance carbon nanotube-based thermoelectric materials (Fig. 24a).[64] A series of six regioregular poly[3-(phenylalkyl)thiophene]s (**46**, P3PATs) bearing phenylalkyl side chains with varying methylene spacer lengths was synthesized *via* Kumada–Tamao–Corriu catalyst-transfer polymerization. Spectroscopic studies reveal efficient energy transfer from P3PATs to single-walled carbon nanotubes (SWCNTs), driven by strong polymer–nanotube interactions, as evidenced by red-shifted UV-vis absorption and pronounced photoluminescence quenching. Morphological analysis shows that increasing the phenylalkyl side-chain length enhances SWCNT wrapping and debundling, leading to reduced bundle diameters and improved dispersion. As a result, the nanocomposites achieve a maximum power factor of 165 ± 22 μW m^{-1} K^{-2}, approximately 2.5 times higher than that of poly(3-hexylthiophene)/SWCNT composites. These findings underscore the crucial role of phenylalkyl side-chain length in regulating polymer–SWCNT interactions, nanocomposite morphology, and thermoelectric performance, providing valuable guidelines for the molecular engineering of high-performance thermoelectric nanocomposites (Fig. 24b).[65]

Developing n-type conjugated polymers with low-lying LUMO energy levels is essential for advancing n-type organic electronics, yet effective strategies to substantially lower the LUMO remain limited. In this work, a strong electron-accepting BDOPV unit was incorporated into the polymer backbone together with fluorine-substituted thiophene donors to afford PB4F2T (**47**), synthesized *via* an atom-economical direct

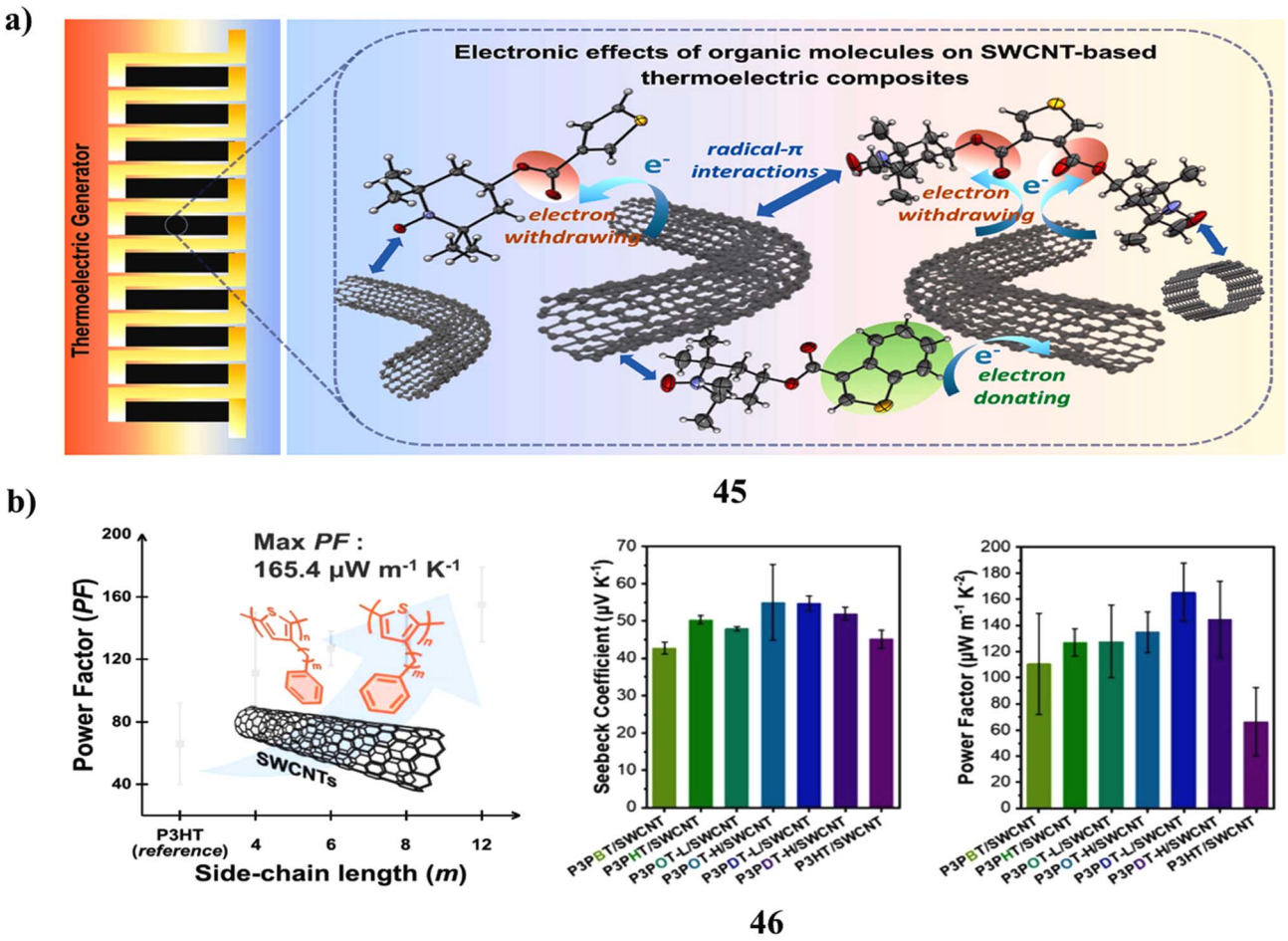

Fig. 24 (a) TEMPO-functionalized thiophenecarboxylates for carbon nanotube-based thermoelectric composites (**45**) Reproduced from ref. 64 with permission from Elsevier Publisher, Copyright 2025. (b) Phenylalkyl-substituted polythiophene/SWCNT nanocomposites with improved thermoelectric performance (**46**) Reproduced from ref. 65 with permission from Elsevier Publisher, Copyright 2025.

arylation monomer-aldol polycondensation strategy. PB4F2T exhibits a LUMO level below −4.0 eV, enabling unipolar n-type charge transport in organic thin-film transistors and efficient n-doping with N-DMBI for organic thermoelectric applications. Organic thermoelectric devices based on PB4F2T demonstrate enhanced performance, achieving an electrical conductivity of 0.90 S cm^{-1} and a power factor of up to 0.50 μW m^{-1} K^{-2}. This work expands the library of unipolar electron-transporting polymer semiconductors by combining strong electron-withdrawing acceptors with fluorinated donor comonomers through an efficient synthetic protocol (Fig. 25a).[66] Efficient thermoelectric conversion of waste heat into electricity requires the concurrent optimization of electrical and thermal transport properties. A comparative theoretical investigation of electron and phonon transport in thiophene- and ethylenedioxythiophene (EDOT)-based molecular wires (**48**) was performed. Substitution of thiophene with ethylenedioxy groups significantly enhances the thermoelectric figure of merit (*ZT*) for molecular wires of identical length. EDOT-based wires exhibit a slower decay of electrical conductance with length and a lower thermal conductance compared to their thiophene counterparts. Although undoped EDOT shows a relatively low room-temperature *ZT*, doping with the electron acceptor *p*-toluenesulfonate markedly increases the Seebeck coefficient and electrical conductance while reducing thermal conductance, yielding a high thermoelectric figure of merit of up to *ZT* = 2.4 (Fig. 25b).[67]

The charge carrier mobility of polythiophene semiconductors (**49**) can be significantly enhanced by heating through a thermotropic mesophase transition, which leads to a pronounced improvement in thin-film structural order. *In situ* structural measurements during heating and cooling reveal that this mesophase transition originates from the melting of interdigitated linear alkyl side chains, specifically quaterdecyl groups. The film morphology and phase behavior throughout the thermal cycle are governed by side-chain conformational changes. Notably, side-chain melting promotes increased backbone ordering, enhanced π–π stacking, and higher charge carrier mobility. Upon cooling, recrystallization of the side chains preserves the mesophase order and the reminder enhanced electrical performance (Fig. 26).[68]

Thiophene-based thermoelectric materials operate on the Seebeck effect, where a temperature gradient induces charge carrier diffusion along the highly conjugated thiophene

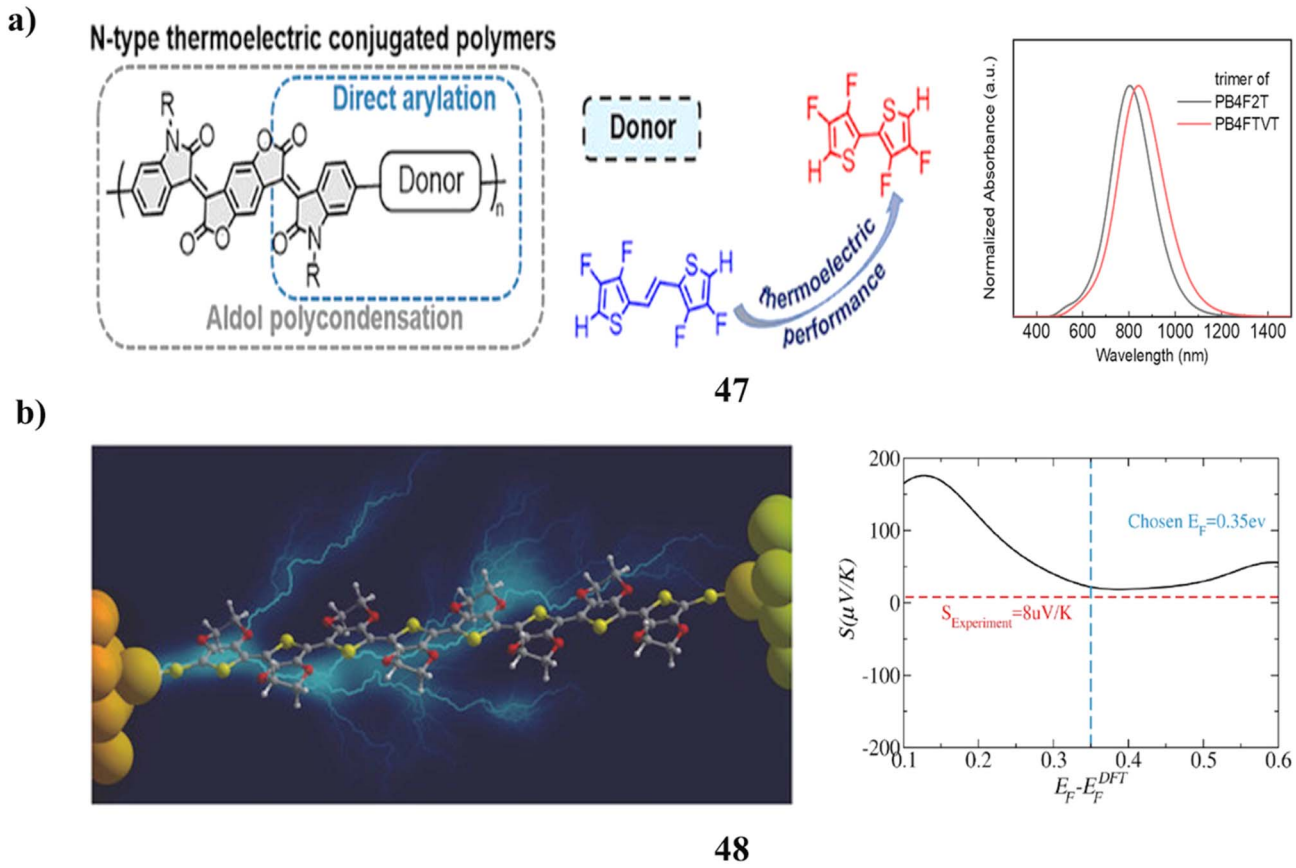

Fig. 25 (a) n-Type benzodifurandione–thiophene polymer thermoelectric materials with low-lying LUMO levels (**47**) Reproduced from ref. 66 with permission from Wiley-VCH Publisher, Copyright 2025. (b) Enhanced thermoelectric performance of thiophene-EDOT molecular wires (**48**) Reproduced from ref. 67 with permission from Wiley-VCH Publisher, Copyright 2018.

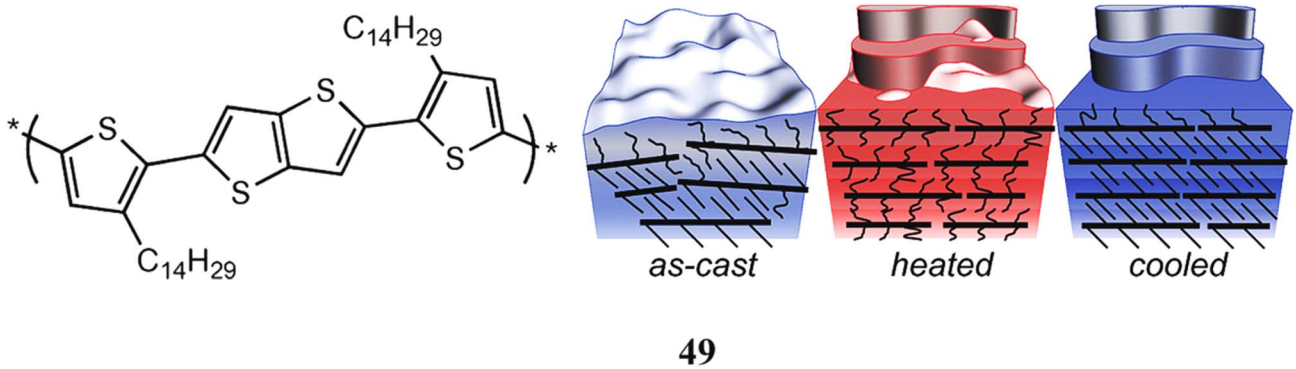

Fig. 26 Mesophase ordering-induced mobility enhancement in thiophene-based copolymers (**49**) Reproduced from ref. 68 with permission from ACS Publisher, Copyright 2008.

backbone, generating electrical voltage, with both p-type and n-type transport achievable through molecular design and doping. Their thermoelectric performance is among the best in organic systems, benefiting from high carrier mobility, strong π–π stacking, donor–acceptor architectures, and effective doping strategies, which together yield high electrical conductivity, moderate-to-high Seebeck coefficients, and competitive power factors at near-room temperature. The detection mechanism is based on the generation of thermovoltage in response to temperature differences, with sensitivity governed by backbone planarity, dopant distribution, interfacial energy filtering, and, in molecular junctions, quantum interference effects. Selectivity arises from tunable electronic structure, side-chain engineering, and controlled electrode coupling, enabling preferential charge transport pathways and, in some cases, selective response to strain, light, or thermal gradients. Key

Table 1 Comparative summary of π-conjugated organic thermoelectric materials, highlighting key performance parameters, device configurations, measurement conditions, and associated advantages and limitations. The table emphasizes structure–property relationships and performance trade-offs across different material classes

Material class	Material/system	Device type	Electrical conductivity ($S\ cm^{-1}$)	Seebeck coefficient ($\mu V\ K^{-1}$)	Power factor ($\mu W\ m^{-1}\ K^{-2}$)	Measurement conditions	Key advantage	Limitation
Fullerene	C_{60} derivatives	Thin film/junction	Moderate	Moderate–high	Moderate	Doped, ambient	Good n-type behavior, air stability	Low conductivity, doping sensitivity
Perylene	PDI-based systems	Bulk/thin film	Moderate	High	Moderate	Controlled doping	Strong electron affinity, stable n-type	Limited mobility
Pyrrole	PPy/CNT composites	Flexible film	High	Moderate	High	Nanocomposite, room temp.	High conductivity, flexible	Structural disorder
Thiophene	PEDOT derivatives	Thin film/flexible device	Very high	Low–moderate	High	Secondary doping	Conductivity, scalable	Lower Seebeck coefficient
Hybrid systems	Polymer/CNT/graphene	Composite	High	Tunable	Very high	Interface-engineered	Energy filtering, enhanced PF	Reproducibility issues

advantages include structural versatility, high charge mobility, good mechanical flexibility, solution processability, and compatibility with flexible, stretchable, and printable thermoelectric devices. However, disadvantages include performance sensitivity to over-doping and structural disorder, stability challenges for n-type thiophene systems, trade-offs between conductivity and Seebeck coefficient, and scalability issues related to reproducible large-area film fabrication.

A comparative analysis of π-conjugated thermoelectric materials highlights distinct advantages and limitations across different systems. Fullerene and perylene-based materials generally exhibit superior n-type behavior and good air stability, but their performance is often constrained by relatively low electrical conductivity and sensitivity to doping conditions. In contrast, pyrrole- and thiophene-based systems offer higher electrical conductivity and better processability, although they may suffer from structural disorder and limited long-term stability. Nanocomposite strategies further enhance performance through interfacial energy filtering and improved charge transport; however, challenges related to reproducibility and scalability persist. Moreover, a critical evaluation of the literature reveals that thermoelectric performance strongly depends on molecular design, doping strategy, and processing conditions. Trade-offs between electrical conductivity and Seebeck coefficient are commonly observed, limiting simultaneous optimization. Additionally, variations in device architecture and measurement conditions complicate direct comparison across studies. Therefore, emphasis should be placed on understanding trends and relative improvements rather than absolute values. These insights underscore the need for standardized evaluation methods. Overall, rational molecular and interfacial design is essential for achieving high-performance organic thermoelectric materials.

A comparative summary of the key thermoelectric parameters and performance characteristics of different π-conjugated material systems is presented in Table 1 to highlight trends and structure–property relationships.

6. Challenges and prospects

Despite significant progress, several challenges continue to limit the practical implementation of organic thermoelectric materials. The simultaneous optimization of electrical conductivity and Seebeck coefficient remains difficult due to their intrinsic trade-off. Achieving high thermoelectric performance at or near room temperature is still challenging for most organic systems. Long-term air, thermal, and operational stability, particularly for n-type materials, requires further improvement. Precise control over molecular doping without inducing structural disorder remains a critical issue. Limited charge carrier mobility in disordered organic films constrains electrical conductivity. Interfacial losses and variability in nanocomposite morphology reduce reproducibility and device reliability. Scalable fabrication of uniform, high-performance films is not yet fully established.

Nevertheless, the prospects for organic thermoelectrics are highly encouraging. Molecular design and synthetic flexibility

enable precise tuning of energy levels and transport pathways. Advanced doping strategies, side-chain engineering, and nanocomposite formation provide effective routes to enhance power factors. Emerging ion-electron coupled systems and interface-engineered materials offer new mechanisms for performance enhancement. The development of flexible, stretchable, and printable thermoelectric devices broadens application potential. Continued integration of structure property insights with device engineering is expected to accelerate progress. Overall, organic thermoelectric materials hold strong promise for sustainable energy harvesting and next-generation flexible electronics.

7. Conclusion

Organic thermoelectric materials represent a rapidly advancing class of energy-harvesting systems with significant potential for sustainable technologies. This work highlights the role of molecular design in tailoring charge transport and thermoelectric efficiency. Fullerene-based materials demonstrate strong thermopower enhancement through interfacial engineering, molecular junction control, and nanostructuring. Perylene derivatives enable high-performance n-type thermoelectrics through effective doping, energy filtering, and ionic–electronic transport control. Pyrrole-based polymers benefit from improved crystallinity, chain alignment, and hierarchical architectures, leading to enhanced electrical conductivity and power factors. Thiophene-based systems offer structural versatility, high carrier mobility, and tunable electronic properties. Nanocomposite formation with carbon nanotubes and graphene significantly improves carrier transport while suppressing thermal conductivity. Doping strategies and side-chain engineering are shown to overcome the conductivity-Seebeck trade-off. Flexible, stretchable, and printable thermoelectric materials expand the scope of practical applications. Light-responsive and hybrid systems introduce new modes of performance control. These advances collectively demonstrate the feasibility of organic thermoelectrics for low-grade waste heat recovery. Continued optimization of molecular structure and interfaces is essential. Integration into scalable device architectures remains a key challenge. Overall, organic thermoelectrics hold strong promise for next-generation energy conversion technologies.

Conflicts of interest

There are no conflicts to declare.

Data availability

No primary research results, software or code have been included and no new data were generated or analysed as part of this review.

Acknowledgements

M. R. thanks Sathyabama Institute of Science and Technology (Deemed to be University), Chennai, Tamil Nadu, India, for providing the necessary infrastructure and instrumentation facilities to carry out this research work.

References

1 A. Raouf, Y. Yu, S. Hao, T. Zhang, M. Ahmad, M. Rashid, I. Ullah, B. Yu and H. Cong, Advancements in thermoelectric hydrogels: structural design and material innovation for biomedical and wearable applications, *J. Mater. Chem. A*, 2025, **13**, 41606–41652.
2 S. Choudhary, V. C. S. Theja, V. A. L. Roy and V. Karthikeyan, 3D additive manufactured thermoelectrics: breaking efficiency barriers in waste heat recovery, *J. Mater. Chem. A*, 2026, **14**, 4306–4322.
3 Q. Wang, Z. Zhou, C. Liu, Y. Zheng, Z. Shi, B. Wei, W. Zhang, C. W. Nan and Y. H. Lin, Advances in oxide thermoelectric materials: strategies, applications and beyond, *Chem. Soc. Rev.*, 2026, **55**, 358–399.
4 S. Liu, H. Li, P. Li, Y. Liu and C. He, Recent Advances in Polyaniline-Based Thermoelectric Composites, *CCS Chem.*, 2021, **3**, 2547–2560.
5 W. Wang, W. Guo, J. Zhu, H. Li, S. Liu, F. Erden, P. Li, M. Yang and C. He, Highly conductive wet-spun PANI/CNTs fibers for wearable energy harvesting and thermal sensing, *J. Colloid Interface Sci.*, 2026, **704**, 139289.
6 C. Xu, S. Yang, P. Li, H. Wang, H. Li and Z. Liu, Wet-spun PEDOT:PSS/CNT composite fibers for wearable thermoelectric energy harvesting, *Compos. Commun.*, 2022, **32**, 101179.
7 D. Kim, H. Kim, J. M. Seo, H. Lee and B. Kang, Recent Trends in Conjugated Polymer-Based Thermoelectrics From Materials to Device, *EcoMat*, 2025, **7**, e70029.
8 C. Lee, Y. Seo, J. Han, J. Hwang and I. Jeon, Perspectives on critical properties of fullerene derivatives for rechargeable battery applications, *Carbon*, 2023, **210**, 118041.
9 U. Kim, J. S. Nam, J. Yoon, J. Han, M. Choi and I. Jeon, Enhanced performance of solution-processed carbon nanotube transparent electrodes in foldable perovskite solar cells through vertical separation of binders by using eco-friendly parylene substrate, *Carbon Energy*, 2024, **6**, e471.
10 A. Alenezi and Y. Alabaiadly, Thermoelectric Cooling in Atmospheric Water Harvesting: A Critical Review of Materials, Design, and Applications, *Energy Nexus*, 2026, 100648.
11 M. H. Rahman Aslam, Advancements in thermoelectric materials and their performance for thermoelectric generators (TEGs): A short review, *Chem. Inorg. Mater.*, 2025, **7**, 100118.
12 S. Zachariah and I. Ravanan, Recent advances in chalcogenides for mid-temperature thermoelectric materials, *J. Alloys Compd.*, 2025, **1043**, 184187.
13 F. A. Shilar and M. Shilar, Thermoelectric materials in building technologies for sustainable construction practices, *Energy Build.*, 2025, **348**, 116426.
14 U. M. B. Al-Naib, A new frontier in thermoelectrics: Emerging materials and pathways to high performance, *Mater. Today Energy*, 2025, **54**, 102076.

15 Y. Zhang, L. Zhang, Z. Wang and G. Chen, Polymer and composite thermoelectric materials with desired mechanical performances for versatile applications, *Energy Chem.*, 2026, **8**, 100181.
16 H. Zhao, T. Sun, L. Cao, M. Shang, Q. Zheng, L. Wang and W. Jiang, Recent Advances in Doping Strategies for N-type Carbon Nanotube-Based Thermoelectric Materials, *ACS Appl. Mater. Interfaces*, 2026, **18**(3), 4611–4631.
17 S. Han, B. Ge and C. Zhou, Solidification Engineering for Thermoelectrics: Figure of Merit and Plasticity, *ACS Appl. Energy Mater.*, 2026, **9**(3), 1335–1345.
18 P. Devi and P. Murugan, Next-Gen II–VI Semiconductor Allotropes: Unlocking Stability and Superior Thermoelectrics via First-Principles Calculations, *J. Phys. Chem. C*, 2026, **130**(4), 1440–1449.
19 X. Yang, Y. Liu, R. Peng, H. Zhang, X. Jiang, J. Zhang, Y. Liu and H. Chen, Discovery of Half-Heusler Alloys with Intrinsically Low Lattice Thermal Conductivity via the Equivalent Valence Electron Principle, *ACS Appl. Mater. Interfaces*, 2026, **18**(4), 6723–6734.
20 C. Tan, P. Peng, Y. Zong, L. Peng and H. Wang, Optimized Thermoelectric Properties in Ta-Doped NbFeSb Alloys via the Lanthanide Contraction Effect for Wearable Applications, *ACS Appl. Mater. Interfaces*, 2026, **18**(3), 5136–5145.
21 S. A. Svatek, V. Sacchetti, L. R. Pérez, B. M. Illescas, L. R. García, G. R. Bollinger, M. T. González, S. Bailey, C. J. Lambert, N. Martín and N. Agraït, Enhanced Thermoelectricity in Metal-[60]Fullerene Graphene Molecular Junctions, *Nano Lett.*, 2023, **23**(7), 2726–2732.
22 L. R. García, A. K. Ismael, C. Evangeli, I. Grace, G. Rubio-Bollinger, K. Porfyrakis, N. Agraït and C. J. Lambert, Molecular design and control of fullerene-based bi-thermoelectric materials, *Future Mater.*, 2016, **15**, 289–293.
23 A. Nadtochiy, V. Kozachenko, O. Korotchenkov and V. Schlosser, Nickel-Fullerene Nanocomposites as Thermoelectric Materials, *Nanomaterials*, 2022, **12**(7), 1163.
24 F. Wu, Y. Shi, W. Zhang, W. Zhao, H. Yang, W. Lai, Y. Lou, Z. Yan, Z. Shi, Z. Ge, X. Wang, L. Fu and B. Xu, Constructing high-performance bulk thermoelectric composites by incorporating uniformly dispersed fullerene sub-nanoclusters, *Acta Mater.*, 2025, **283**, 120540.
25 L. Qiu, J. Liu, R. Alessandri, X. Qiu, M. Koopmans, R. W. A. Havenith, S. J. Marrink, R. C. Chiechi, L. J. A. Koster and J. C. Hummelen, Enhancing doping efficiency by improving host-dopant miscibility for fullerene-based n-type thermoelectrics, *J. Mater. Chem. A*, 2017, **5**, 21234–21241.
26 J. Liu, L. Qiu, G. Portale, S. Torabi, M. C. A. Stuart, X. Qiu, M. Koopmans, R. C. Chiechi, J. C. Hummelen and L. J. A. Koster, Side-chain effects on N-type organic thermoelectrics: A case study of fullerene derivatives, *Nano Energy*, 2018, **52**, 183–191.
27 L. Yu, J. Xu, B. Peng, G. Qin and G. Su, Anisotropic Optical, Mechanical, and Thermoelectric Properties of Two-Dimensional Fullerene Networks, *J. Phys. Chem. Lett.*, 2022, **13**(50), 11622–11629.
28 R. Wang, G. Dong, S. Wang, G. Fu and J. Wang, Thermoelectric properties of fullerene-based junctions: a first-principles study, *Phys. Chem. Chem. Phys.*, 2016, **18**, 28117–28124.
29 P. Zhou, G. Li and M. Sun, Electronic, optoelectronic, and thermoelectric properties of single molecular devices of 2D fullerenes with zigzag graphene nanoribbons as electrodes, *Phys. Chem. Chem. Phys.*, 2023, **25**, 31615–31627.
30 B. Mortazavi, Structural, electronic, thermal and mechanical properties of C_{60}-based fullerene two-dimensional networks explored by first-principles and machine learning, *Carbon*, 2023, **213**, 118293.
31 L. Wang, Z. Zhang, L. Geng, T. Yuan, Y. Liu, J. Guo, L. Fang, J. Qiu and S. Wang, Solution-printable fullerene/TiS_2 organic/inorganic hybrids for high-performance flexible n-type thermoelectrics, *Energy Environ. Sci.*, 2018, **11**, 1307–1317.
32 H. Zhou, Y. Zheng, X. Wang, H. R. Tan and J. Xu, Photoresponsive Thermoelectric Materials Derived from Fullerene-C_{60} PEDOT Hybrid Polymers, *ACS Appl. Energy Mater.*, 2020, **3**(7), 6726–6734.
33 Z. Wang, N. Jin, L. Lu, S. Ao, Y. Zhang, S. Qi and T. Jia, Highly efficient solar-thermal thermoresponsive hydrogel based on a fullerene derivative for water purification and energy harvesting, *J. Mater. Chem. C*, 2025, **13**, 10817–10824.
34 S. K. Lee, M. Buerkle, R. Yamada, Y. Asai and H. Tada, Thermoelectricity at the molecular scale: a large Seebeck effect in endohedral metallofullerenes, *Nanoscale*, 2015, **7**, 20497–20502.
35 Y. Jia, Q. Jiang, B. Wang, Z. Ma, D. Zhao, N. Zheng, J. Zhou, P. Liu, D. Hu and Y. Ma, Utilizing perylene diimmide as dopant to improve thermoelectric performance of PEDOT:PSS films, *Compos. Commun.*, 2021, **27**, 100844.
36 C. Chou, S. Fang, P. Lin, W. Wu, S. Hong, J. Lin, K. Wong and C. Liu, Tuning thermoelectric performance with N-annulated perylene-based small molecules and single-walled carbon nanotube nanocomposite films, *Mater. Today Commun.*, 2024, **38**, 102129.
37 J. Liang, S. Sun, S. Huang, J. Jin, D. Zheng, J. Luo and D. Liu, Boosting thermoelectric performance of carbon nanotube-based materials and devices by radical-containing molecules, *Mater. Today Commun.*, 2023, **35**, 106317.
38 Q. Jiang, H. Sun, D. Zhao, F. Zhang, D. Hu, F. Jiao, L. Qin, V. Linseis, S. Fabiano, X. Crispin, Y. Ma and Y. Cao, High Thermoelectric Performance in n-Type Perylene Bisimide Induced by the Soret Effect, *Adv. Mater.*, 2020, **32**, 2002752.
39 G. Wu, Z. Zhang, Y. Li, C. Gao, X. Wang and G. Chen, Exploring High-Performance n-Type Thermoelectric Composites Using Amino-Substituted Rylene Dimides and Carbon Nanotubes, *ACS Nano*, 2017, **11**(6), 5746–5752.
40 N. Wu, Y. Zhang, C. Wang, P. M. Slattum, X. Yang and L. Zang, Thermoactivated Electrical Conductivity in Perylene Diimide Nanofiber Materials, *J. Phys. Chem. Lett.*, 2017, **8**(1), 292–298.
41 J. D. Yuen, V. A. Pozdin, A. T. Young, B. L. Turner, I. D. Giles, J. Naciri, S. A. Trammell, P. T. Charles, D. A. Stenger and M. A. Daniele, Perylene-diimide-based n-type

semiconductors with enhanced air and temperature stable photoconductor and transistor properties, *Dyes Pigm.*, 2020, **174**, 108014.

42 L. Wang, F. Liu, C. Jin, T. Zhang and Q. Yin, Preparation of polypyrrole/graphene nanosheets composites with enhanced thermoelectric properties, *RSC Adv.*, 2014, **4**, 46187–46193.

43 Q. Zheng, C. Tseng, M. Lin, J. Lin, S. Tung, Y. Cheng and C. Liu, High-performance ladder-type conjugated polymer/carbon nanotube nanocomposites blended with elastomers for stretchable thermoelectric thin films, *J. Mater. Chem. C*, 2024, **12**, 7446–7455.

44 X. Tang, T. Liu, H. Li, D. Yang, L. Chen and X. Tang, Notably enhanced thermoelectric properties of lamellar polypyrrole by doping with β-naphthalene sulfonic acid, *RSC Adv.*, 2017, **7**, 20192–20200.

45 M. Culebras, Y. Byun, J. Jang, T. K. Lee, D. Choi, A. Serafin, M. N. Collins, J. S. Cho and C. Cho, Enhanced Thermoelectric Performance in Polypyrrole-Based Multilayer Nanoarchitectures via Thermal Reduction, *ACS Appl. Energy Mater.*, 2024, **7**(6), 2351–2361.

46 K. Wang, P. Lin, Y. Lin, S. Tung, W. Chen and C. Liu, Tunable Thermoelectric Performance of the Nanocomposites Formed by Diketopyrrolopyrrole/Isoindigo-Based Donor–Acceptor Random Conjugated Copolymers and Carbon Nanotubes, *ACS Appl. Mater. Interfaces*, 2023, **15**(48), 56116–56126.

47 Y. Kuang, M. Yang, L. Pan, G. Ye, S. Shao, C. Duan and J. Liu, Thermoelectric Performance of n-Type Conjugated Polymer Based on a Quinoidal Unit of Benzodipyrrolidone, *Chem. Mater.*, 2024, **36**(22), 11075–11083.

48 J. Park, Y. Lee, M. Kim, Y. Kim, A. Tripathi, Y. Kwon, J. Kwak and H. Y. Woo, Closely Packed Polypyrroles via Ionic Cross-Linking: Correlation of Molecular Structure–Morphology–Thermoelectric Properties, *ACS Appl. Mater. Interfaces*, 2020, **12**(1), 1110–1119.

49 Y. Li, C. Gao, X. Fan and L. Yang, *In-situ* pulse electropolymerization of pyrrole on single-walled carbon nanotubes for thermoelectric composite materials, *Chem. Eng. J.*, 2022, **443**, 136536.

50 S. Wang, F. Liu, C. Gao, T. Wan, L. Wang, L. Wang and L. Wang, Enhancement of the thermoelectric property of nanostructured polyaniline/carbon nanotube composites by introducing pyrrole unit onto polyaniline backbone via a sustainable method, *Chem. Eng. J.*, 2019, **370**, 322–329.

51 K. K. Garg, S. Pandey, L. Pandey, A. Kumar, A. Rana, S. Madan, N. G. Sahoo, S. K. Dhawan and R. K. Singh, Copper-catalyzed plastic waste synthesized graphene nanosheets/polypyrrole nanocomposites for efficient thermoelectric applications, *Next Sustainability*, 2025, **5**, 100081.

52 I. H. Jung, C. T. Hong, U. Lee, Y. H. Kang, K. Jang and S. Y. Cho, High Thermoelectric Power Factor of a Diketopyrrolopyrrole-Based Low Bandgap Polymer via Finely Tuned Doping Engineering, *Sci. Rep.*, 2017, **7**, 44704.

53 Z. Liu, J. Sun, H. Song, Y. Pan, Y. Song, Y. Zhu, Y. Yao, F. Huang and C. Zuo, High performance polypyrrole/SWCNTs composite film as a promising organic thermoelectric material, *RSC Adv.*, 2021, **11**, 17704–17709.

54 K. Ueda, R. Fukuzaki, T. Ito, N. Toyama, M. Muraoka, T. Terao, K. Manabe, T. Hirai, C. Wu, S. Chuang, S. Kawano and M. Murat, A Highly Conductive n-Type Coordination Complex with Thieno[3,2-*b*]thiophene Units: Facile Synthesis, Orientation, and Thermoelectric Properties, *J. Am. Chem. Soc.*, 2022, **144**(41), 18744–18749.

55 W. B. Chang, C. Mai, M. Kotiuga, J. B. Neaton, G. C. Bazan and R. A. Segalman, Controlling the Thermoelectric Properties of Thiophene-Derived Single-Molecule Junctions, *Chem. Mater.*, 2014, **26**(24), 7229–7235.

56 P. Lin, K. Yaginuma, Y. Liu, J. Lin, S. Tung, H. Matsumoto, M. Ashizawa and C. Liu, Synthesis and Thermoelectric Properties of Nickel Tetrathiolate Metallopolymers, *ACS Appl. Energy Mater.*, 2025, **8**(18), 13499–13509.

57 Y. Hu, X. Liu, F. Jiang, W. Zhou, C. Liu, X. Duan and J. Xu, Functionalized Poly(3,4-ethylenedioxy bithiophene) Films for Tuning Electrochromic and Thermoelectric Properties, *J. Phys. Chem. B*, 2017, **121**(39), 9281–9290.

58 X. Fan, S. Deng, X. Cao, B. Meng, J. Hu and J. Liu, Isomers of n-Type Poly(thiophene-*alt*-*co*-thiazole) for Organic Thermoelectrics, *ACS Appl. Mater. Interfaces*, 2024, **16**(35), 46741–46749.

59 R. Almughathawi, S. Hou, Q. Wu, Z. Liu, W. Hong and C. Lambert, Conformation and Quantum-Interference-Enhanced Thermoelectric Properties of Diphenyl Diketopyrrolopyrrole Derivatives, *ACS Sens.*, 2021, **6**(2), 470–476.

60 M. J. A. Navarro, O. Z. Arteaga, S. R. Galindo, J. Guo, A. Peredeventsv, E. G. Fernández, J. S. Reparaz, M. Ramos, C. Müller, J. Martín, M. M. Torrent, J. L. Segura and M. C. Quiles, Low-bandgap oligothiophene-naphthalimide oligomeric semiconductors for thermoelectric applications, *J. Mater. Chem. C*, 2025, **13**, 6922–6932.

61 Y. Huang, G. Xiao, J. Chen, Y. Shi, Z. Zhang, H. Hu, D. Yuan, Y. Yao, K. Yang and Z. Zeng, n-Type polymer semiconductors based on conformation-locked π-extended bithieno[3,4-*c*]pyrrole-4,6-dione (BTPD) acceptor units for organic thermoelectrics, *J. Mater. Chem. C*, 2025, **13**, 17970–17978.

62 S. Wu, W. Xing, M. Zhu, Y. Zou, Y. Sun, W. Xu and D. Zhu, Doped thieno[3,4-*b*]thiophene-based copolymers for p-type organic thermoelectric materials, *J. Mater. Chem. C*, 2021, **9**, 4158–4163.

63 N. Raveendran, T. Ghosh, V. Ignatious, V. Darshan, N. Jacob, B. Deb and C. Vijayakumar, Thermoelectric properties of self-assembled thiophene derivatives: effect of molecular structure on doping efficiency and Fermi level alignment, *Mater. Today Energy*, 2023, **34**, 101296.

64 S. Sun, M. Fan, Y. Wang, J. Zhang, J. Jin, H. Xiao, L. Wang and D. Liu, Unveiling electronic effects of TEMPO-containing thiophenecarboxylates on carbon nanotube-based thermoelectric composites, *Mater. Today Chem.*, 2025, **46**, 102753.

65 T. Fujita, M. Matsuda, P. Lin, C. Chou, J. Lin, C. Liu and T. Higashihara, Improved thermoelectric performance of phenylalkyl-substituted polythiophene/single-walled carbon

nanotube nanocomposites, *J. Colloid Interface Sci.*, 2025, **699**, 138299.

66 R. Gao, Y. Guo, C. Xu, W. Dong, Y. Xu, Y. Han, Y. Deng and Y. Geng, n-Type Polymer Thermoelectric Materials Based on Benzodifurandione and F-Substituted Thiophene Derivatives Synthesized via Direct Arylation and Aldol Polycondensation, *Macromol. Chem. Phys.*, 2025, **266**(14), 70002.

67 M. Famili, I. M. Grace, Q. Al-Galiby, H. Sadeghi and C. J. Lambert, Toward High Thermoelectric Performance of Thiophene and Ethylenedioxythiophene (EDOT) Molecular Wires, *Adv. Funct. Mater.*, 2018, **28**(15), 1703135.

68 D. M. DeLongchamp, R. Joseph Kline, Y. Jung, E. K. Lin, D. A. Fischer, D. J. Gundlach, S. K. Cotts, A. J. Moad, M. L. J. Richter, F. Toney, M. Heeney and I. McCulloch, Molecular Basis of Mesophase Ordering in a Thiophene-Based Copolymer, *Macromolecules*, 2008, **41**(15), 5709–5715.